AD NUMBER

AD886554

LIMITATION CHANGES

TO:

Approved for public release; distribution is unlimited.

FROM:

Distribution authorized to U.S. Gov't. agencies only; Test and Evaluation; AUG 1971. Other requests shall be referred to Armament Development and Test Center, Attn: DLDG, Eglin AFB, FL 32542.

AUTHORITY

ADTC ltr, 4 Aug 1976

AEDC-TR-71-140
AFATL-TR-71-92

Cy.2

SEPARATION CHARACTERISTICS OF THE SUU-51 LASER-GUIDED DISPENSER MUNITION FROM THE F-4C AIRCRAFT

Robert H. Roberts

ARO, Inc.

August 1971

PROPERTY OF U.S AIR FORCE
AEDC LIBRARY
F40600-72-C-0003

PROPULSION WIND TUNNEL FACILITY

ARNOLD ENGINEERING DEVELOPMENT CENTER

AIR FORCE SYSTEMS COMMAND

ARNOLD AIR FORCE STATION, TENNESSEE

NOTICES

When U. S. Government drawings specifications, or other data are used for any purpose other than a definitely related Government procurement operation, the Government thereby incurs no responsibility nor any obligation whatsoever, and the fact that the Government may have formulated, furnished, or in any way supplied the said drawings, specifications, or other data, is not to be regarded by implication or otherwise, or in any manner licensing the holder or any other person or corporation, or conveying any rights or permission to manufacture, use, or sell any patented invention that may in any way be related thereto.

Qualified users may obtain copies of this report from the Defense Documentation Center.

References to named commercial products in this report are not to be considered in any sense as an endorsement of the product by the United States Air Force or the Government.

SEPARATION CHARACTERISTICS OF THE SUU-51 LASER-GUIDED DISPENSER MUNITION FROM THE F-4C AIRCRAFT

Robert H. Roberts
ARO, Inc.

FOREWORD

The work reported herein was sponsored by the Air Force Armament Development and Test Center (ADTC), Air Force Armament Laboratory (DLGC), Air Force Systems Command (AFSC), under Program Element 64724F, Project 1120, Task 09.

The test results presented were obtained by ARO, Inc. (a subsidiary of Sverdrup & Parcel and Associates, Inc.), contract operator of the Arnold Engineering Development Center (AEDC), AFSC, Arnold Air Force Station, Tennessee, under Contract F40600-72-C-0003. The test was conducted from April 16 to 19, 1971, under ARO Project No. PC0140. The manuscript was submitted for publication on May 24, 1971.

This technical report has been reviewed and is approved.

George F. Garey
Lt Colonel, USAF
AF Representative, PWT
Directorate of Test

Joseph R. Henry
Colonel, USAF
Director of Test

ABSTRACT

Tests were conducted in the Aerodynamic Wind Tunnel (4T) using 0.05-scale models to investigate the separation characteristics of the SUU-51 Laser-Guided Dispenser Munition (LGDM) from Triple Ejection Rack and Multiple Ejection Rack locations on the inboard and centerline pylons, respectively, of the F-4C aircraft. Captive-trajectory store separation data were obtained at Mach numbers from 0.66 to 0.90, angles of attack from 0.3 to 2.1, and a simulated altitude of 5000 ft. At selected test conditions, parent-aircraft dive angles of 30 and 45 deg were simulated. Free-stream force and moment data were also obtained on the SUU-51 (LGDM) model at Mach numbers from 0.66 to 0.95 at store angles of attack from -6 to 20 deg. Generally, the store initially separated from the parent aircraft without store-to-parent contact. However, most of the trajectories were terminated after short time intervals because of a rapid pitch and yaw motion of the store. This termination was the result of limitations imposed by the test installation, such as sting-to-parent-aircraft contact, a store support system travel limit, or a balance load limit.

CONTENTS

APPENDIXES

I. ILLUSTRATIONS

Figure

NOMENCLATURE

BL	Aircraft buttock line from plane of symmetry, in., model scale
b	Store reference dimension, ft full scale
C_A	Store axial-force coefficient, axial force/$q_\infty S$
C_m	Store pitching-moment coefficient, referenced to the store center of gravity (cg), pitching moment/$q_\infty Sb$
C_{m_q}	Store pitch-damping derivative, $dC_m/d(qb/2V_\infty)$
C_n	Store yawing-moment coefficient, referenced to the store cg, yawing moment/$q_\infty Sb$
C_{n_r}	Store yaw-damping derivative, $dC_n/d(rb/2V_\infty)$
FS	Aircraft fuselage station, in., model scale
F_Z	MER/TER ejector force, lb
H	Pressure altitude, ft
I_{xx}	Full-scale moment of inertia about the store X_B axis, slug-ft^2
I_{xz}	Full-scale product of inertia, X_B-Z_B axis, slug-ft^2

I_{yy} Full-scale moment of inertia about the store Y_B axis, slug-ft^2

I_{zz} Full-scale moment of inertia about the store Z_B axis, slug-ft^2

M_∞ Free-stream Mach number

$\overline{m}$ Full-scale store mass, slugs

p_∞ Free-stream static pressure, psfa

q Store angular velocity about the Y_B axis, radians/sec

q_∞ Free-stream dynamic pressure, 0.7 $p_\infty M_\infty^2$, psf

r Store angular velocity about the Z_B axis, radians/sec

S Store reference area, ft^2, full scale

t Real trajectory time from initiation of trajectory, sec

V_∞ Free-stream velocity, ft/sec

WL Aircraft waterline from reference horizontal plane, in., model scale

X Separation distance of the store cg parallel to the flight axis system X_F direction, ft, full scale measured from the prelaunch position

X_{cg} Full-scale cg location, ft from nose of store

X_L Ejector piston location relative to the store cg, positive forward of store cg, ft full scale

Y Separation distance of the store cg parallel to the flight axis system Y_F direction, ft, full scale measured from the prelaunch position

Z Separation distance of the store cg parallel to the flight-axis system Z_F direction, ft, full scale measured from the prelaunch position

Z_E Ejector stroke length, ft, full scale

α Parent-aircraft or store model angle of attack relative to the free-stream velocity vector, deg

θ Angle between the store longitudinal axis and its projection in the X_F-Y_F plane, positive when store nose is raised as seen by pilot, deg

$\bar{\theta}$ Simulated parent-aircraft climb angle. Angle between the flight direction and the earth horizontal, deg, positive for increasing altitude

ψ Angle between the projection of the store longitudinal axis in the X_F-Y_F plane and the X_F axis, positive when the store nose is to the right as seen by the pilot, deg

FLIGHT-AXIS SYSTEM COORDINATES

Directions

X_F Parallel to the free-stream wind vector, positive direction is forward as seen by the pilot

Y_F Perpendicular to the X_F and Z_F directions, positive direction is to the right as seen by the pilot

Z_F In the aircraft plane of symmetry, perpendicular to the free-stream wind vector, positive direction is downward

The flight-axis system origin is coincident with the aircraft cg and remains fixed with respect to the parent aircraft during store separation. The X_F, Y_F, and Z_F coordinate axes do not rotate with respect to the initial flight direction and attitude.

STORE BODY-AXIS SYSTEM COORDINATES

Directions

X_B Parallel to the store longitudinal axis, positive direction is upstream in the prelaunch position

Y_B Perpendicular to the store longitudinal axis, and parallel to the flight-axis system X_F-Y_F plane when the store is at zero roll angle, positive direction is to the right looking upstream when the store is at zero yaw and roll angles

Z_B Perpendicular to both the X_B and Y_B axes, positive direction is downward as seen by the pilot when the store is at zero pitch and roll angles

The store body-axis system origin is coincident with the store cg and moves with the store during separation from the parent airplane. The X_B, Y_B, and Z_B coordinate axes rotate with the store in pitch, yaw, and roll so that mass moments of inertia about the three axes are not time-varying quantities.

SECTION I
INTRODUCTION

This investigation was conducted in the Aerodynamic Wind Tunnel (4T) of the Propulsion Wind Tunnel Facility to obtain captive-trajectory store-separation data for the SUU-51 (LGDM) store when released from various F-4C inboard and centerline multiple carriage configurations. Separation trajectories with the folded-fin configuration were initiated from the launch positions with simulated ejector forces acting on the store. If a trajectory was of sufficient length to reach the position where the fins could be deployed, the open-fin configuration was used to obtain additional data, initiating from the chosen store location along the original trajectory. The criterion for fin deployment was a clearance of at least 1.5 ft between the rack and the aft end of the store. Although a number of trajectories met this criterion, many of them were terminated a very short time after fin deployment because of limitations imposed by the test installation, e.g., sting-to-parent-aircraft contact, store support system travel limits, or a balance load limit. These short open-fin-configuration trajectory continuations are not presented.

To simulate the separation trajectories, 0.05-scale models of the SUU-51 (LGDM) and F-4C were employed. The store models were attached to the Captive Trajectory System (CTS) in the 4T wind tunnel. Flight conditions simulated were Mach numbers from 0.66 to 0.90, an altitude of 5000 ft, and parent-aircraft angles of attack from 0.3 to 2.1 deg. At selected test conditions, parent-aircraft dive angles of 30 and 45 deg were simulated. Free-stream static stability data for the store model were obtained at Mach numbers from 0.66 to 0.95 at store angles of attack from -6 to 20 deg.

SECTION II
APPARATUS

2.1 TEST FACILITY

The Aerodynamic Wind Tunnel (4T) is a closed-loop, continuous flow, variable-density tunnel in which the Mach number can be varied from 0.2 to 1.3. At all Mach numbers, the stagnation pressure can be varied from 200 to 3400 psfa. The test section is 4 ft square and 12.5 ft long with perforated, variable porosity (0.5- to 10-percent open) walls. It is completely enclosed in a plenum chamber from which the air can be evacuated, allowing part of the tunnel airflow to be removed through the perforated walls of the test section.

For store separation testing, two separate and independent support systems are used to support the models. The parent aircraft model is inverted in the test section and supported by an offset sting attached to the main pitch sector. The store model is supported by the CTS which extends down from the tunnel top wall and provides store movement (six degreees of freedom) independent of the parent-aircraft model. An isometric drawing of a typical store separation installation is shown in Fig. 1, Appendix I.

Also shown in Fig. 1 is a block diagram of the computer control loop used during captive trajectory testing. The analog system and the digital computer work as an integrated

unit and, utilizing required input information, control the store movement during a trajectory. Store positioning is accomplished by use of six individual d-c electric motors. Maximum translational travel of the CTS is ±15 in. from the tunnel centerline in the lateral and vertical directions and 36 in. in the axial direction. Maximum angular displacements are ±45 deg in pitch and yaw and ±360 deg in roll. A more complete description of the test facility can be found in the Test Facilities Handbook.[1] A schematic showing the test section details and the location of the models in the tunnel is shown in Fig. 2.

2.2 TEST ARTICLES

The test articles were 0.05-scale models of the F-4C parent aircraft and the SUU-51 (LGDM) store. A sketch showing the basic dimensions of the F-4C parent model is shown in Fig. 3. For this test, only the left wing and fuselage centerline of the F-4C were equipped for store separation. Details and dimensions of the pylons are shown in Fig. 4. The surfaces of the fuselage centerline and wing inboard pylons are inclined at a 2.5- and 1.0-deg nose-down angle, respectively, with respect to the aircraft waterline.

The Triple Ejection Rack (TER) and Multiple Ejection Rack (MER) were mounted on the inboard and centerline pylons, respectively, and matched to the 30-in. suspension lugs of the pylons. Details and dimensions of the TER and MER are shown in Figs. 5 and 6, respectively.

Details and dimensions of the SUU-51 (LGDM) store model are shown in Fig. 7. A dimensional sketch of the 370-gal dummy fuel tank used to simulate the desired aircraft configuration is shown in Fig. 8. Aircraft/weapons loading nomenclature used for describing the configurations is given in Fig. 9, and the loading configurations for which trajectory data were obtained are shown in Fig. 10.

2.3 INSTRUMENTATION

A five-component, internal strain-gage balance was used to obtain the force and moment data on the SUU-51 (LGDM) model. Translational and angular positions of the store model were obtained from the CTS analog outputs. An angular position indicator on the main pitch sector was used to determine the parent-model angle of attack. The MER and TER were instrumented with a touch wire at each station which aided in the positioning of the sting-mounted store model at the launch position on the rack. The system was also electrically connected to automatically stop the CTS movement if the store model or sting contacted the rack or the aircraft-model surface.

---

[1]Test Facilities Handbook (Eighth Edition). "Propulsion Wind Tunnel Facility, Vol. 5." Arnold Engineering Development Center, December 1969.

SECTION III
TEST DESCRIPTION

3.1 TEST CONDITIONS

Separation trajectory data were obtained at Mach numbers from 0.66 to 0.90. Tunnel dynamic pressure was 500 psf at all Mach numbers, and tunnel stagnation temperature was maintained near 100°F. Tunnel conditions were held constant at the desired Mach number and stagnation pressure while data for each trajectory were obtained. The trajectories were terminated when the store or sting contacted the parent-aircraft model or when a CTS limit was reached.

3.2 TRAJECTORY DATA ACQUISITION

To obtain a trajectory, test conditions were established in the tunnel and the parent model was positioned at the desired angle of attack. The store model was then oriented to a position corresponding to the store carriage location. After the store was set at the desired initial position, operational control of the CTS was switched to the digital computer which controlled the store movement during the trajectory through commands to the CTS analog system (see block diagram, Fig. 1). Data from the wind tunnel, consisting of measured model forces and moments, wind tunnel operating conditions, and CTS rig positions, were input to the digital computer for use in the full-scale trajectory calculations.

The digital computer was programmed to solve the six-degree-of-freedom equations to calculate the angular and linear displacements of the store relative to the parent aircraft pylon. In general, the program involves using the last two successive measured values of each static aerodynamic coefficient to predict the magnitude of the coefficients over the next time interval of the trajectory. These predicted values are used to calculate the new position and attitude of the store at the end of the time interval. The CTS is then commanded to move the store model to this new position and the aerodynamic loads are measured. If these new measurements agree with the predicted values, the process is continued over another time interval of the same magnitude. If the measured and predicted values do not agree within the desired precision, the calculation is redone over a time interval one-half the previous value. This process is repeated until a complete trajectory has been obtained.

In applying the wind tunnel data to the calculations of the full-scale store trajectories, the measured forces and moments are reduced to coefficient form and then applied with proper full-scale store dimensions and flight dynamic pressure. Dynamic pressure was calculated using a flight velocity equal to the free-stream velocity component plus the components of store velocity relative to the aircraft, and a density corresponding to the simulated altitude.

The initial portion of each launch trajectory incorporated simulated ejector forces in addition to the measured aerodynamic forces acting on the store. The ejector force function for the SUU-51 (LGDM) store is presented in Fig. 11. The ejector force was

considered to act perpendicular to the rack mounting surface. The locations of the applied ejector forces and other full-scale store parameters used in the trajectory calculations are listed in Table I, Appendix II.

3.3 CORRECTIONS

Balance, sting, and support deflections caused by the aerodynamic loads on the store models were accounted for in the data reduction program to calculate the true store-model angles. Corrections were also made for model weight tares to calculate the net aerodynamic forces on the store model.

3.4 PRECISION OF DATA

The trajectory data are subject to error from several sources including tunnel conditions, balance measurements, extrapolation tolerances allowed in the predicted coefficients, computer inputs, and CTS positioning control. Maximum error in the CTS position control was ±0.05 in. for the translational settings and ±0.15 deg for angular displacement settings in pitch and yaw. Extrapolation tolerances were ±0.10 for each of the aerodynamic coefficients. The maximum uncertainties in the full-scale position data caused by the balance precision limitations are given in Table II.

The estimated uncertainty in setting Mach number was no greater than ±0.003, and the uncertainty in parent-model angle of attack was estimated to be ±0.1 deg.

SECTION IV
RESULTS AND DISCUSSION

Data obtained during this test consisted of separation trajectories of the SUU-51 (LGDM) from the F-4C inboard and centerline multiple carriage configurations. Data showing the linear and angular displacements of the store relative to the mate position on the racks or pylons are presented as functions of full-scale trajectory time in Figs. 12 through 20. Positive X, Y, and Z displacements (as seen by the pilot) are forward, to the right (inboard), and down, respectively. Positive changes in pitch and yaw (as seen by the pilot) are nose up and nose right (inboard), respectively. Unless otherwise noted in the following discussion, termination of the trajectories after only a short time interval was a result of limitations imposed by the CTS system, such as sting-to-parent aircraft contact, a CTS travel limit, or a balance load limit.

Figures 12 and 13 present trajectory data for load configuration 2. At M_∞ = 0.82 and 0.90, all trajectories were terminated when the aft portion of the SUU-51 (LGDM) store contacted the TER.

Figure 12 presents data showing the effect of parent-aircraft dive angle on separation trajectories from the inboard TER. No significant effects are noted.

For several of the separation trajectories, the aerodynamic moments were referenced to a point forward of the cg of the SUU-51 (LGDM). This 1-cal (1.3333 ft full scale) forward shift in moment center (F) from the normal position (N) was a stabilizing maneuver which simulated an increased fin area of the store. Figure 13 presents data comparing these two moment-center locations. The only effect of a forward shift in moment center on separation trajectories was a slightly reduced rate of pitch and yaw.

The small effect of dive angle and moment-center shift shown for configuration 2 was consistent throughout the remaining load configurations; thus, the remaining separation trajectories are presented with Mach number, and corresponding angle of attack, as the only variable.

Figures 14 through 17, and Figs. 18 and 19, present data for launches from TER stations on the wing inboard pylon, and MER stations on the centerline pylon, respectively. The launch sequences from the MER and TER (see Fig. 9) are such that configurations 3, 5, and 8 represent mirror images of launches from the right wing or right-hand side of the MER, and all other configurations represent left-wing or left-hand-side launches. Almost all separation trajectories presented exhibit an initial nose down pitch motion, which is more rapid at the higher Mach numbers, and an outboard yaw motion. All stores separated without contacting the parent aircraft. However, the rapid pitch and yaw motions caused many of these trajectories to be terminated after a short time interval because of CTS limitations.

Figure 20 presents data showing the effect of open fins on the separation trajectories for selected launch conditions. The stabilizing effect of the deployed fins can be seen for each configuration.

Free-stream static stability data are presented in Figs. 21 and 22 for the SUU-51 (LGDM) folded-fin and open-fin models, respectively. The stabilizing effectiveness of the open fins is markedly reduced at angles of attack greater than 10 deg.

APPENDIXES

I. ILLUSTRATIONS
II. TABLES

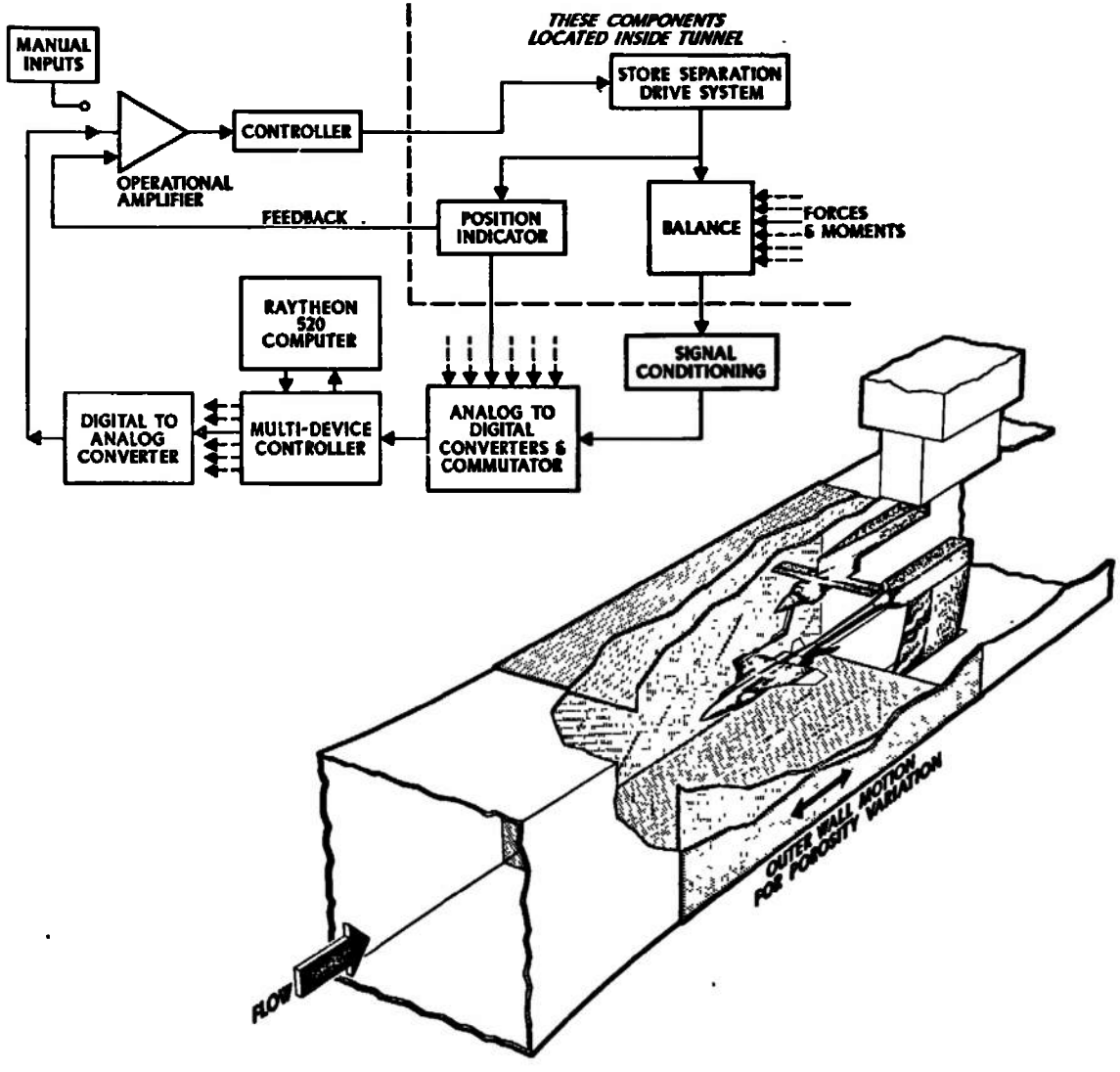

Fig. 1 Isometric Drawing of a Typical Store Separation Installation and a Block Diagram of the Computer Control Loop

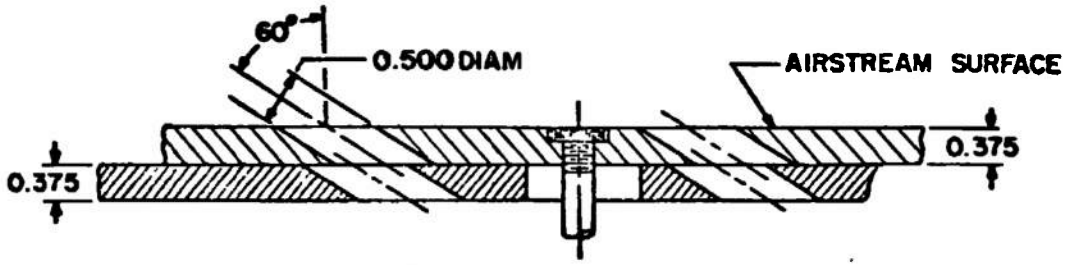

TYPICAL PERFORATED WALL CROSS SECTION

NOTE: TUNNEL STATIONS AND DIMENSIONS ARE IN INCHES

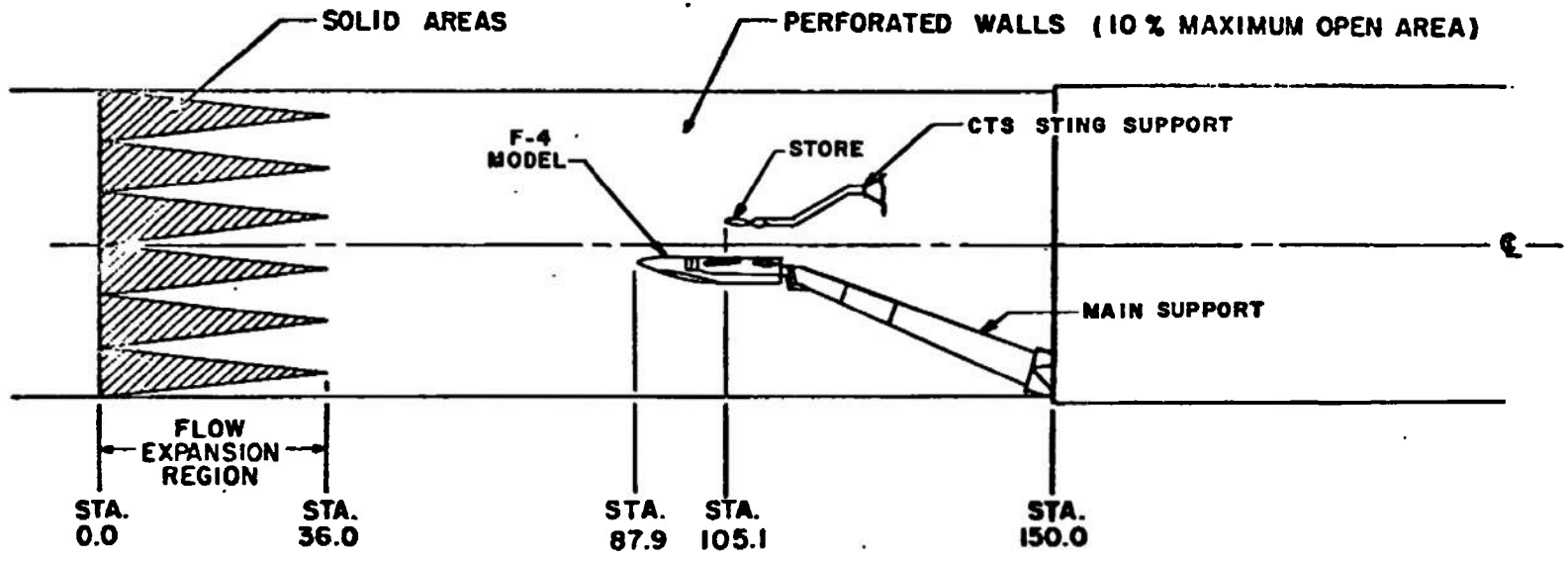

Fig. 2 Schematic of the Tunnel Test Section Showing Model Location

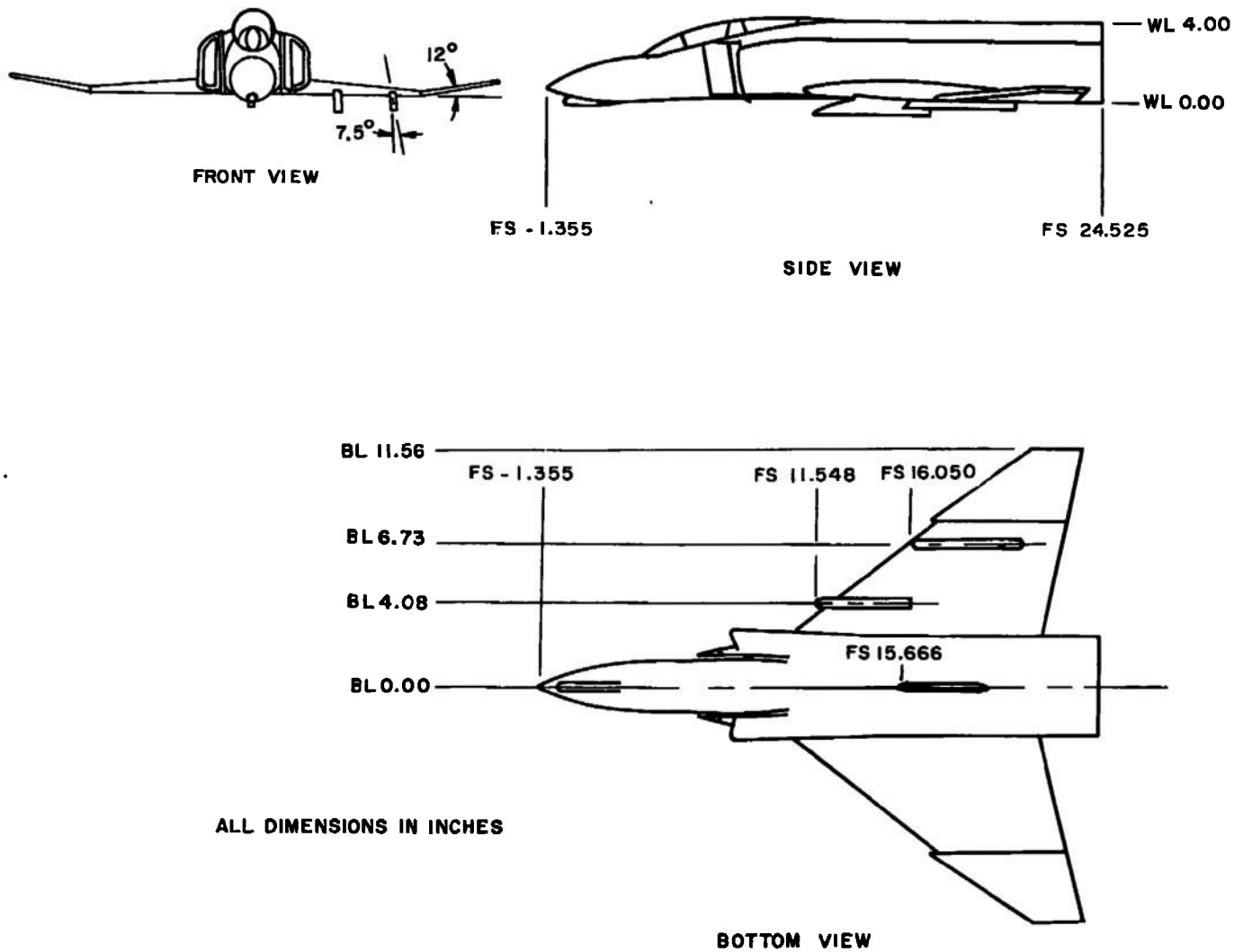

Fig. 3 Sketch of the F-4C Parent-Aircraft Model

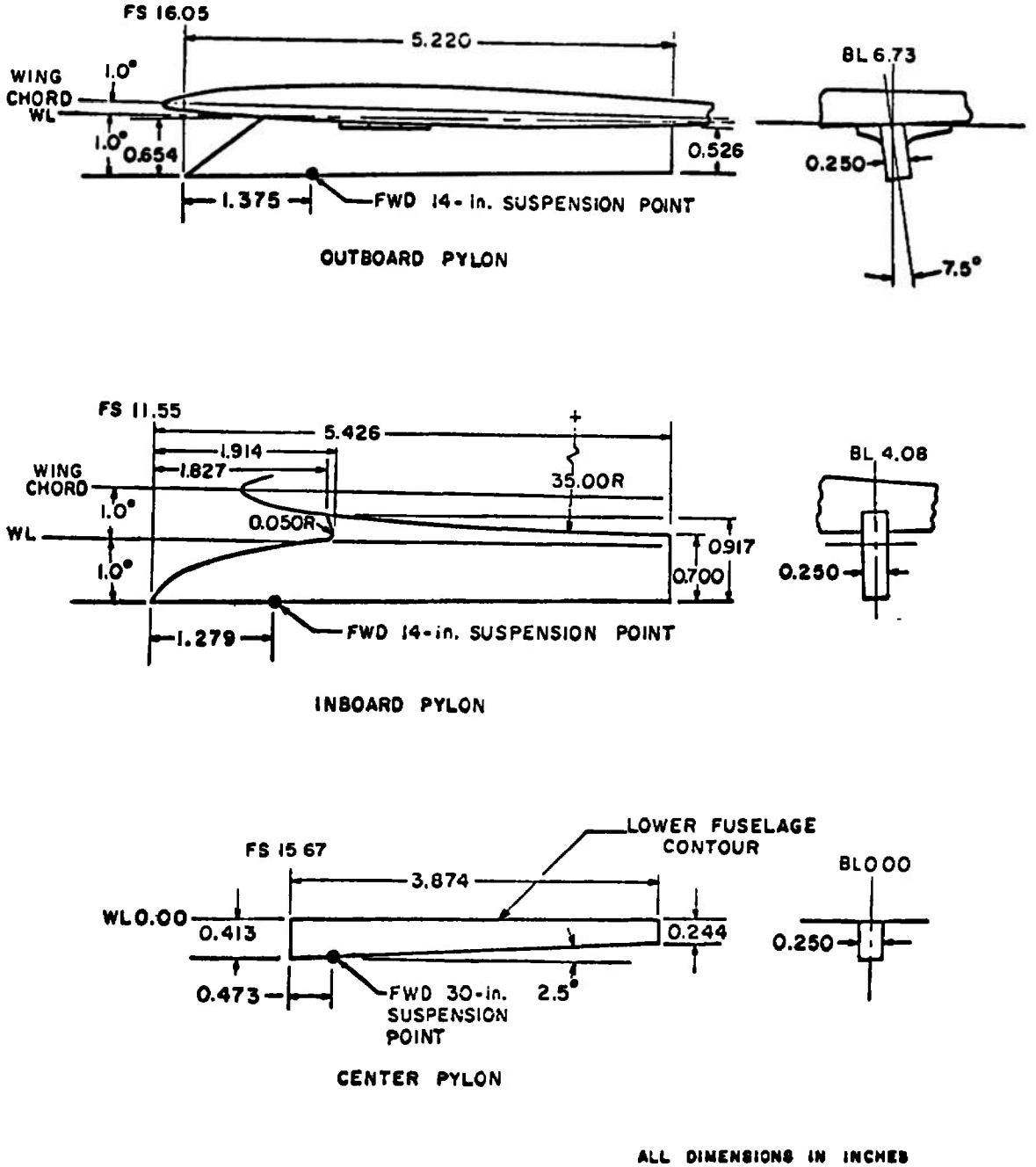

Fig. 4 Details and Dimensions of the F-4C Pylon Models

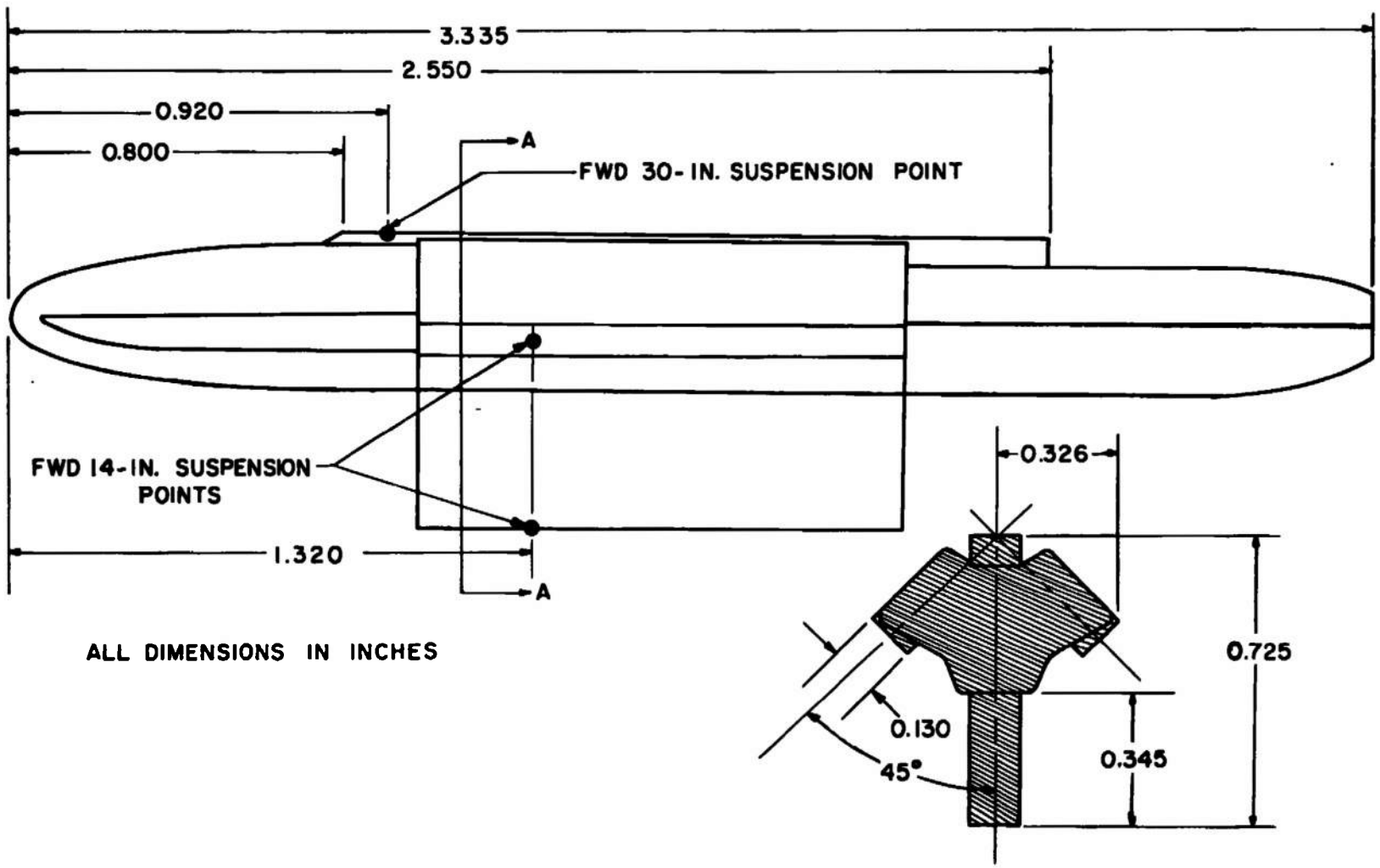

Fig. 5 Details and Dimensions of the TER Model

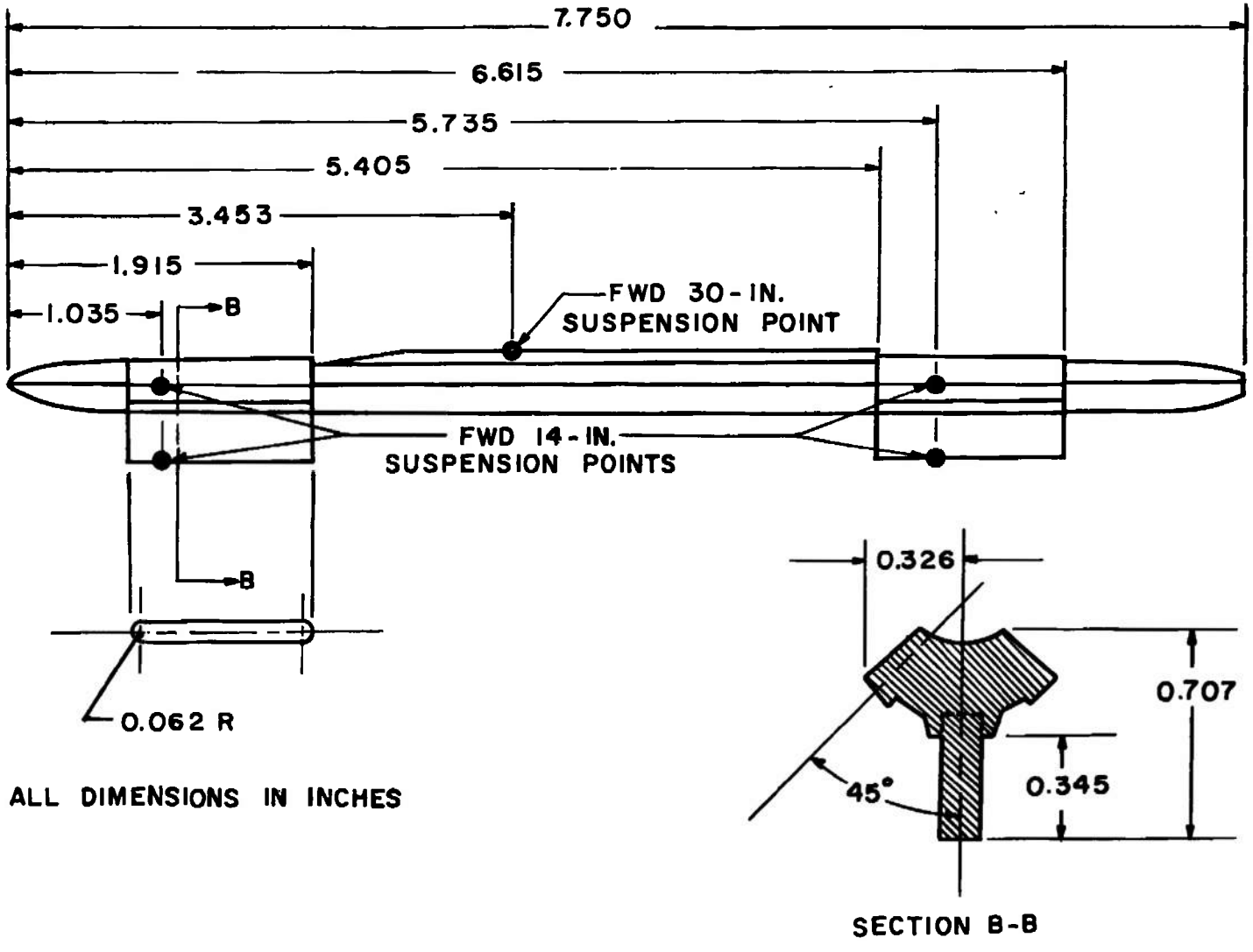

Fig. 6 Details and Dimensions of the MER Model

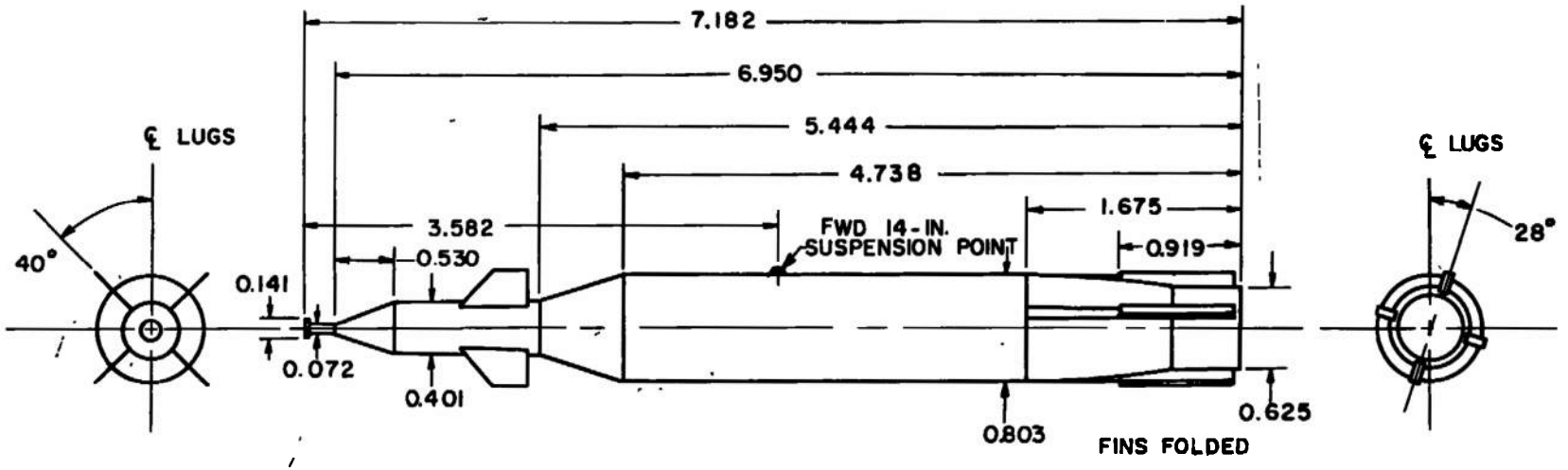

ALL DIMENSIONS IN INCHES

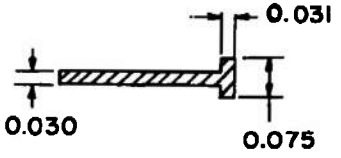

SECTION A-A

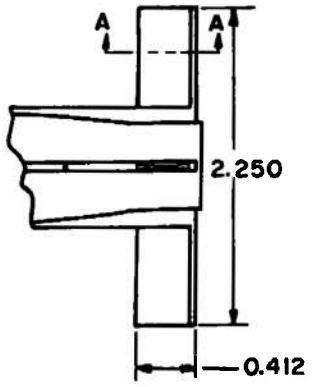

FINS DEPLOYED

Fig. 7 Details and Dimensions of the SUU-51 (LGDM) Model

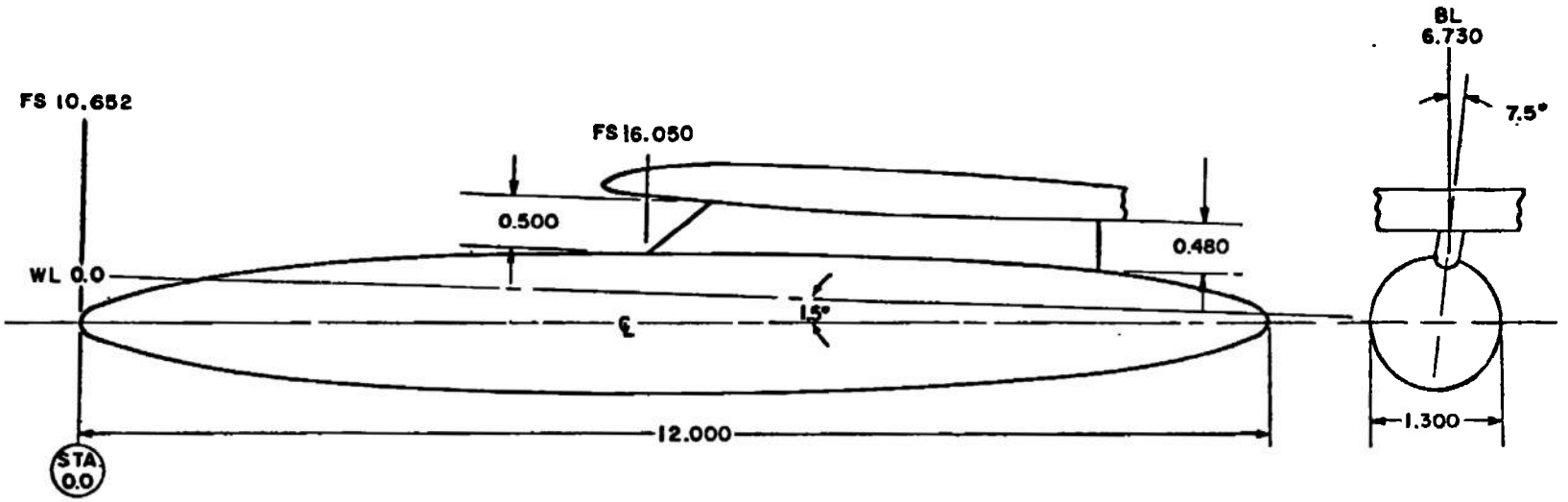

ALL DIMENSIONS AND MODEL STATIONS IN INCHES

BODY CONTOUR, TYPICAL BOTH ENDS

STATION	BODY DIAM	STATION	BODY DIAM
0.000	0.000	2.500	1.116
0.025	0.100	2.750	1.156
0.050	0.144	3.000	1.190
0.150	0.258	3.250	1218
0.250	0.340	3.500	1.242
0.500	0.498	3.750	1.260
0.750	0.622	4.000	1.274
1.000	0 724	4.250	1.286
1.250	0 812	4.500	1.294
1.500	0.890	4.750	1298
1.750	0.958	5.000	1300
2000	1.016	6.000	1.300
2.250	1.070		

Fig. 8 Details and Dimensions of the 370-gal Dummy Fuel Tank

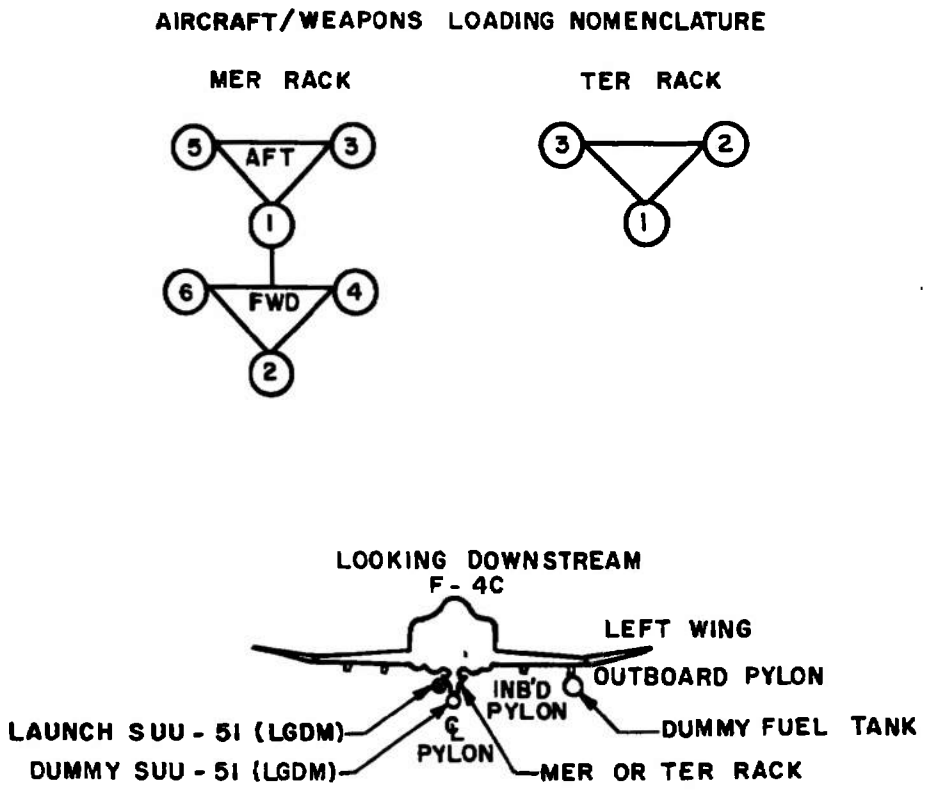

Fig. 9 Aircraft/Weapons Loading Nomenclature

CONFIGURATION 1

℄ PYLON	INBOARD PYLON	OUTBOARD PYLON
MER STA. 1: EMPTY	TER STA. 1: LAUNCH	370 GAL. FUEL TANK
MER STA.2: EMPTY	TER STA. 2: DUMMY	
MER STA.3: EMPTY	TER STA.3: DUMMY	
MER STA.4: EMPTY		
MER STA. 5: EMPTY		
MER STA. 6: EMPTY		

CONFIGURATION 2

℄ PYLON	INBOARD PYLON	OUTBOARD PYLON
MER STA 1: EMPTY	TER STA. 1: EMPTY	370 GAL FUEL TANK
MER STA. 2. DUMMY	TER STA. 2: LAUNCH	
MER STA. 3: EMPTY	TER STA 3: DUMMY	
MER STA. 4: EMPTY		
MER STA 5: EMPTY		
MER STA 6: EMPTY		

CONFIGURATION 3

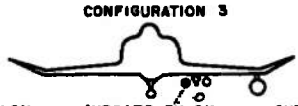

℄ PYLON	INBOARD PYLON	OUTBOARD PYLON
MER STA 1: EMPTY	TER STA. 1: EMPTY	370 GAL. FUEL TANK
MER STA 2: DUMMY	TER STA. 2: DUMMY	
MER STA 3: EMPTY	TER STA. 3: LAUNCH	
MER STA. 4. EMPTY		
MER STA 5: EMPTY		
MER STA 6: EMPTY		

CONFIGURATION 4

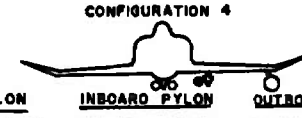

℄ PYLON	INBOARD PYLON	OUTBOARD PYLON
MER STA. 1: EMPTY	TER STA. 1 EMPTY	370 GAL FUEL TANK
MER STA. 2: EMPTY	TER STA 2. EMPTY	
MER STA 3: DUMMY	TER STA. 3: LAUNCH	
MER STA. 4: EMPTY		
MER STA 5: DUMMY		
MER STA 6: EMPTY		

CONFIGURATION 5

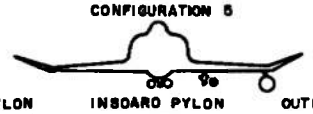

℄ PYLON	INBOARD PYLON	OUTBOARD PYLON
MER STA. 1: EMPTY	TER STA. 1: EMPTY	370 GAL. FUEL TANK
MER STA. 2: EMPTY	TER STA. 2 LAUNCH	
MER STA 3: DUMMY	TER STA. 3: EMPTY	
MER STA. 4: EMPTY		
MER STA. 5 . DUMMY		
MER STA. 6 : EMPTY		

CONFIGURATION 6

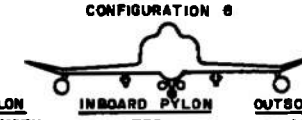

℄ PYLON	INBOARD PYLON	OUTBOARD PYLON
MER STA. 1: EMPTY	TER	370 GAL. FUEL TANK
MER STA 2: LAUNCH		
MER STA 3: DUMMY		
MER STA 4: EMPTY		
MER STA. 5: DUMMY		
MER STA. 6: EMPTY		

CONFIGURATION 7

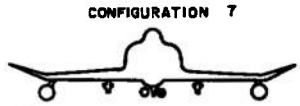

℄ PYLON	INBOARD PYLON	OUTBOARD PYLON
MER STA 1: EMPTY	TER	370 GAL. FUEL TANK
MER STA. 2: EMPTY		
MER STA. 3: LAUNCH		
MER STA. 4: EMPTY		
MER STA. 5: DUMMY		
MER STA. 6 . EMPTY		

CONFIGURATION 8

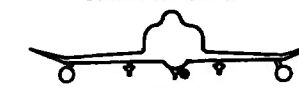

℄ PYLON	INBOARD PYLON	OUTBOARD PYLON
MER STA 1 : EMPTY	TER	370 GAL. FUEL TANK
MER STA. 2: EMPTY		
MER STA 3 . LAUNCH		
MER STA 4 . EMPTY		
MER STA. 5 . EMPTY		
MER STA 6: EMPTY		

Fig. 10 Schematic of Aircraft/Weapons Loading Configurations

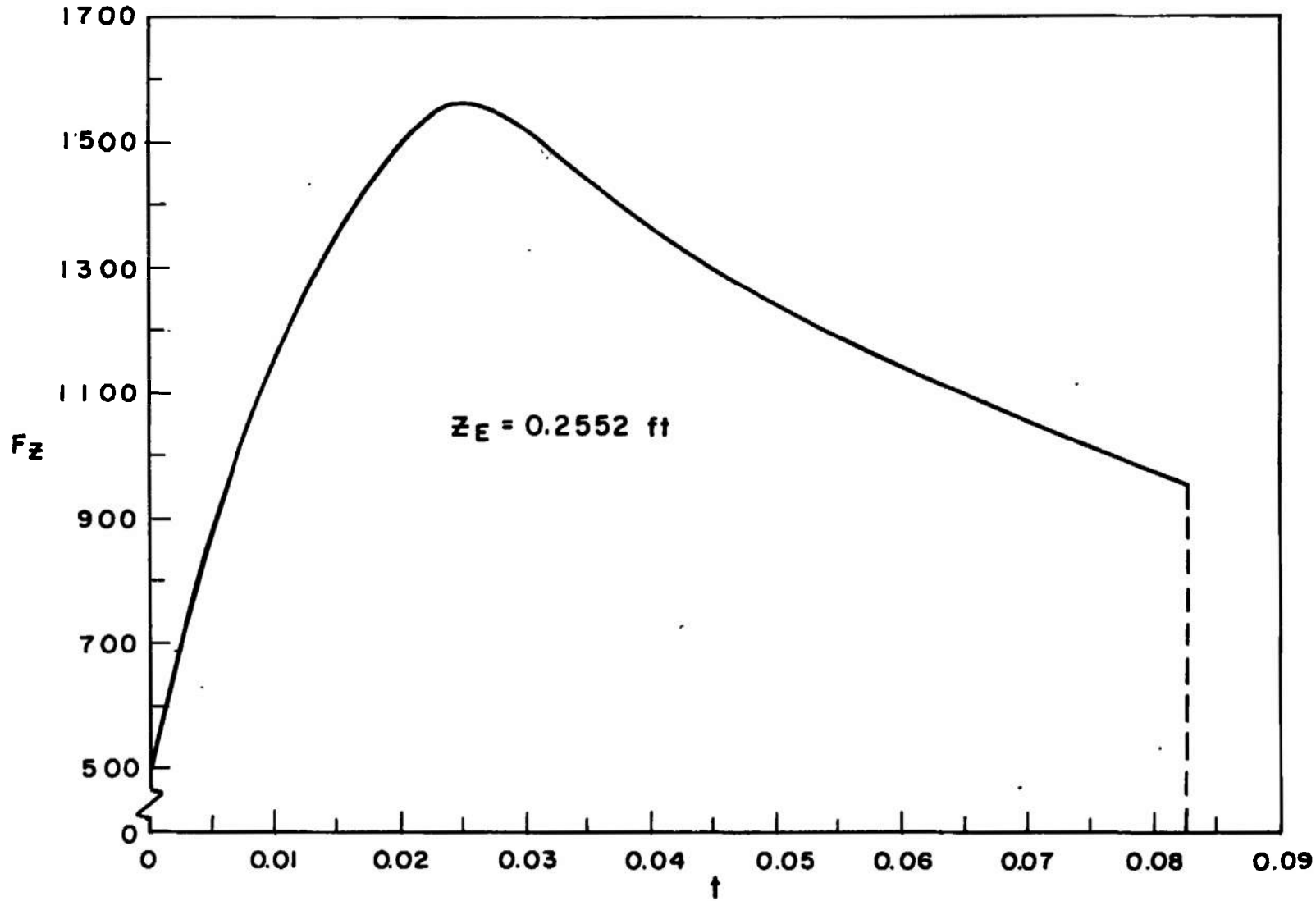

Fig. 11 TER and MER Ejector Force Function

SYM	CONF	M_∞	α	H	$\bar{\theta}$
□	2	0.66	2.1	5000	0
○	2	0.66	2.1	5000	-30

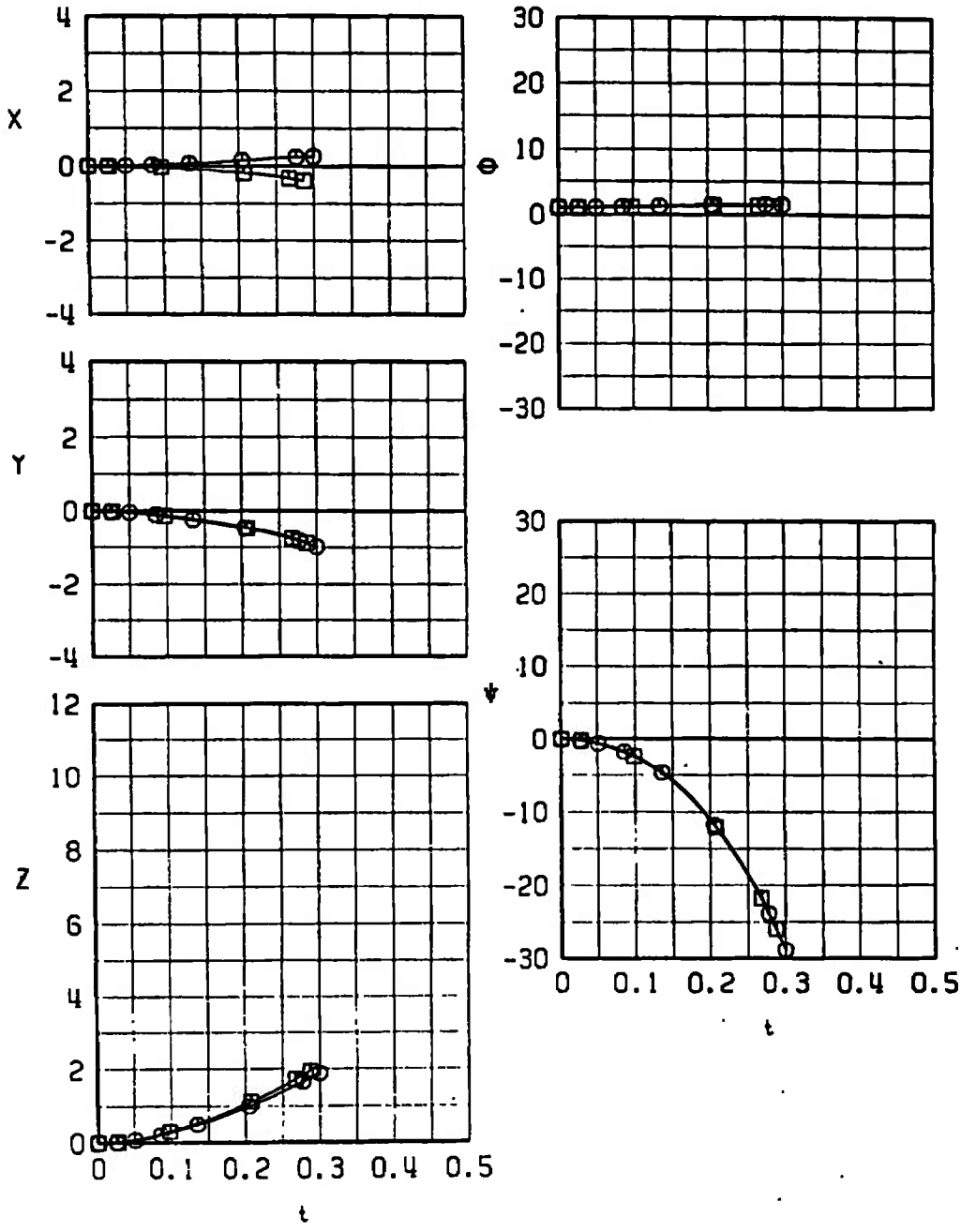

a. $M_\infty = 0.66$

Fig. 12 Effect of Parent Aircraft Dive Angle on Separation Trajectories from Left Wing TER, Station 2; Fins Folded

SYM	CONF	M_∞	α	H	$\bar{\theta}$
□	2	0.74	1.3	5000	0
○	2	0.74	1.3	5000	-30
△	2	0.74	1.3	5000	-45

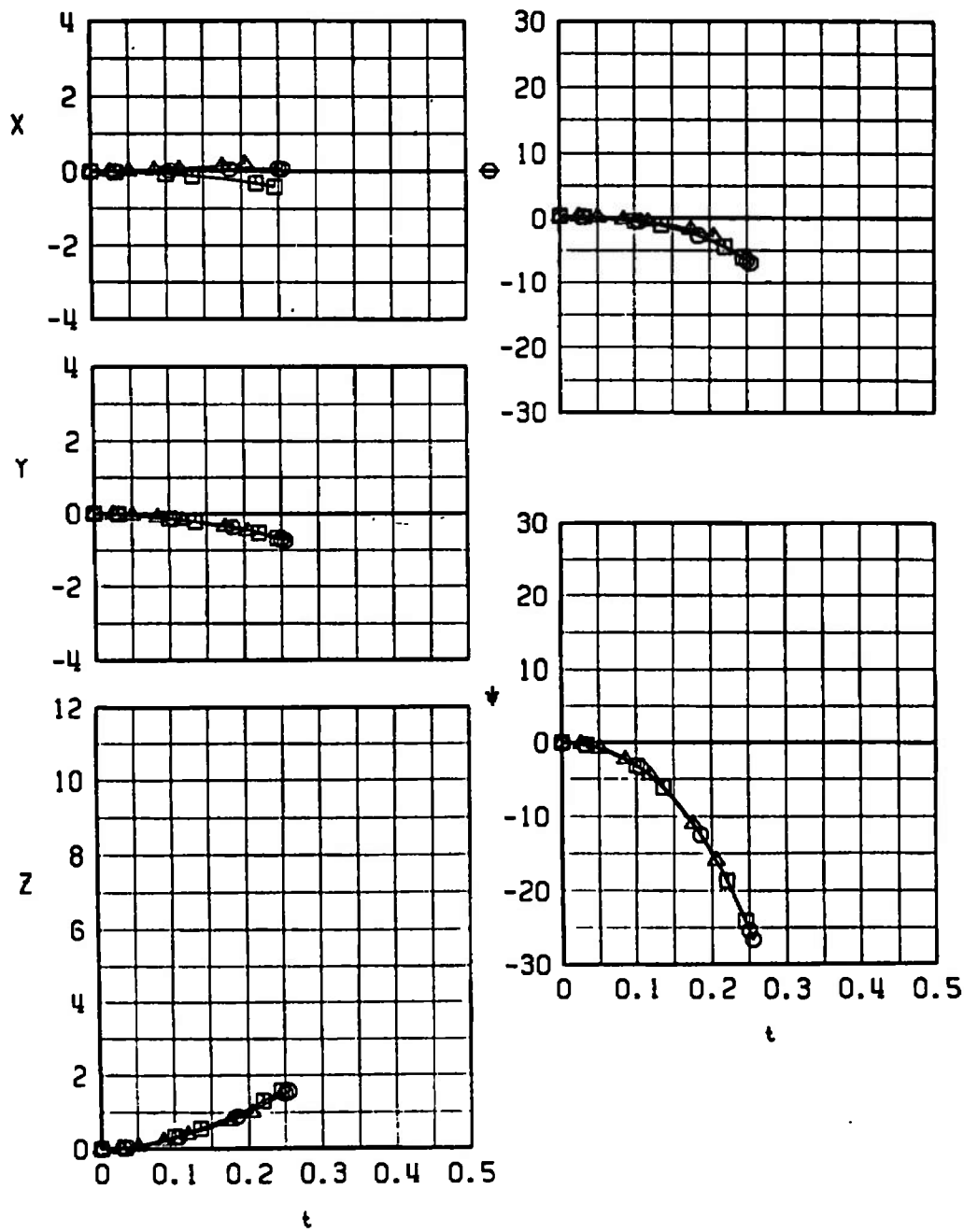

b. $M_\infty = 0.74$

Fig. 12 Continued

SYM	CONF	M_∞	α	H	$\bar{\theta}$
□	2	0.82	0.7	5000	0
○	2	0.82	0.7	5000	-30
△	2	0.82	0.7	5000	-45

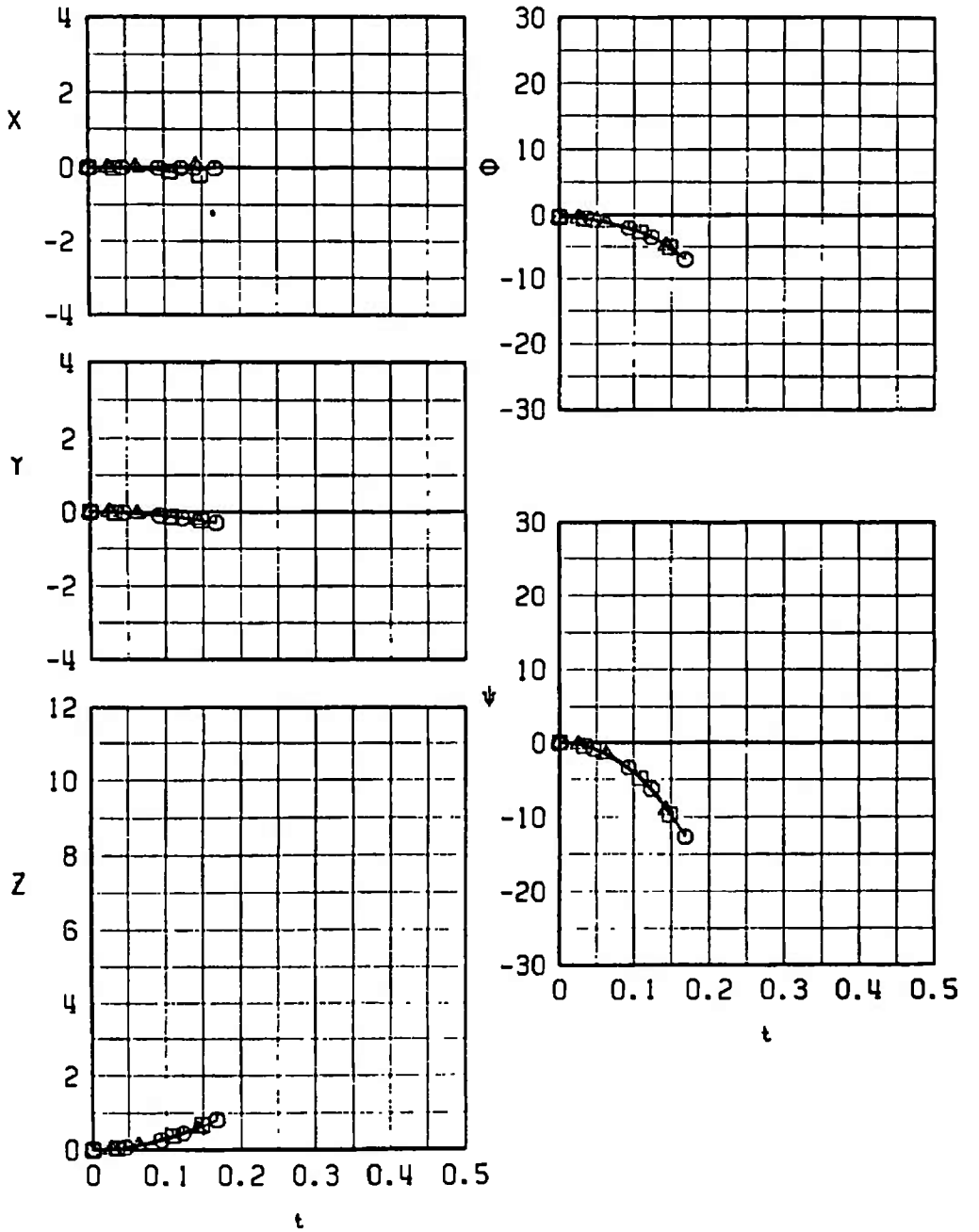

c. $M_\infty = 0.82$

Fig. 12 Continued

SYM	CONF	M_∞	α	H	$\bar{\theta}$
□	2	0.90	0.3	5000	0
○	2	0.90	0.3	5000	-30
△	2	0.90	0.3	5000	-45

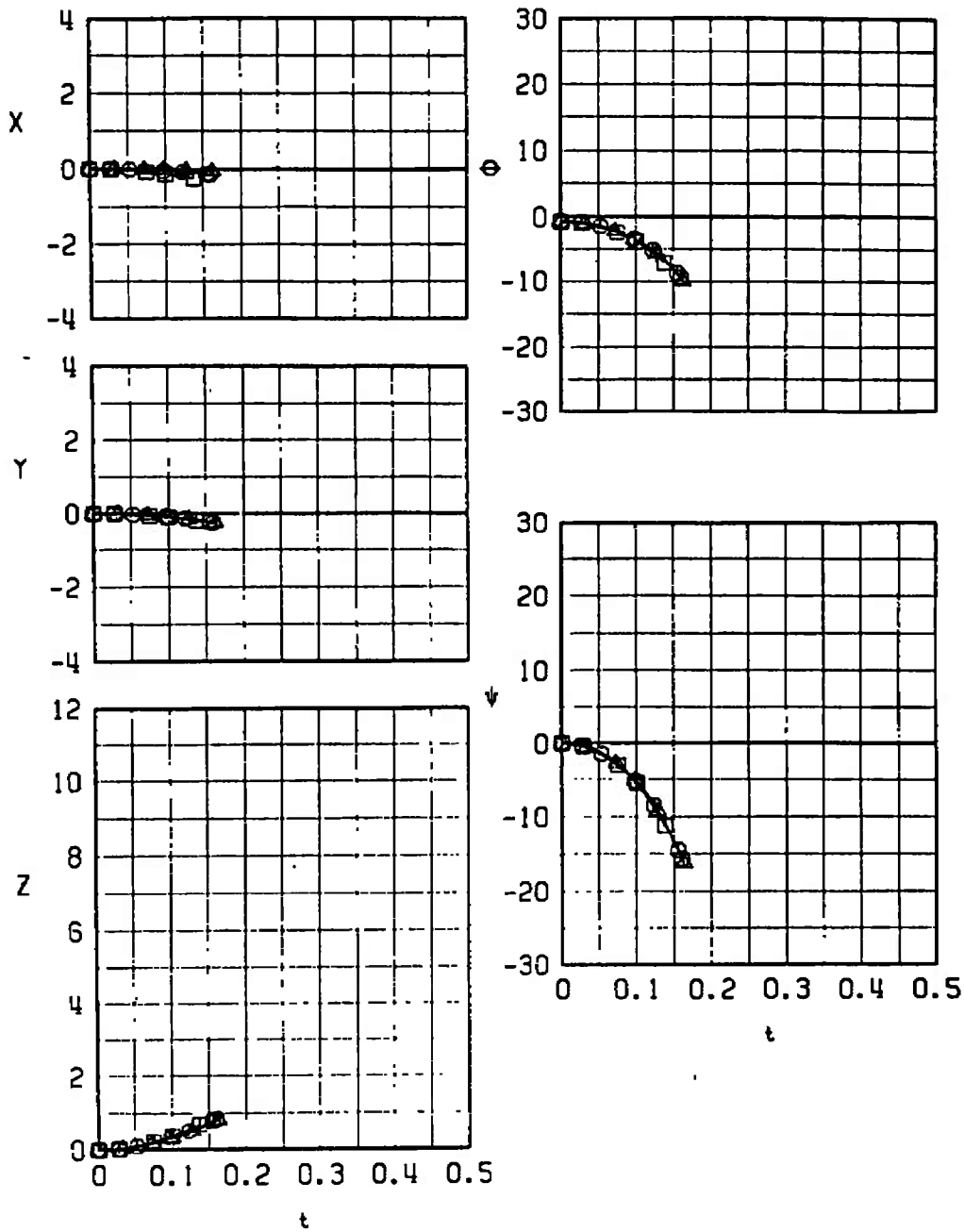

d. $M_\infty = 0.90$

Fig. 12 Concluded

SYM	CONF	M_∞	α	H	$\bar{\theta}$	MOMENT CENTER
□	2	0.66	2.1	5000	- 30	N
○	2	0.66	2.1	5000	- 30	F

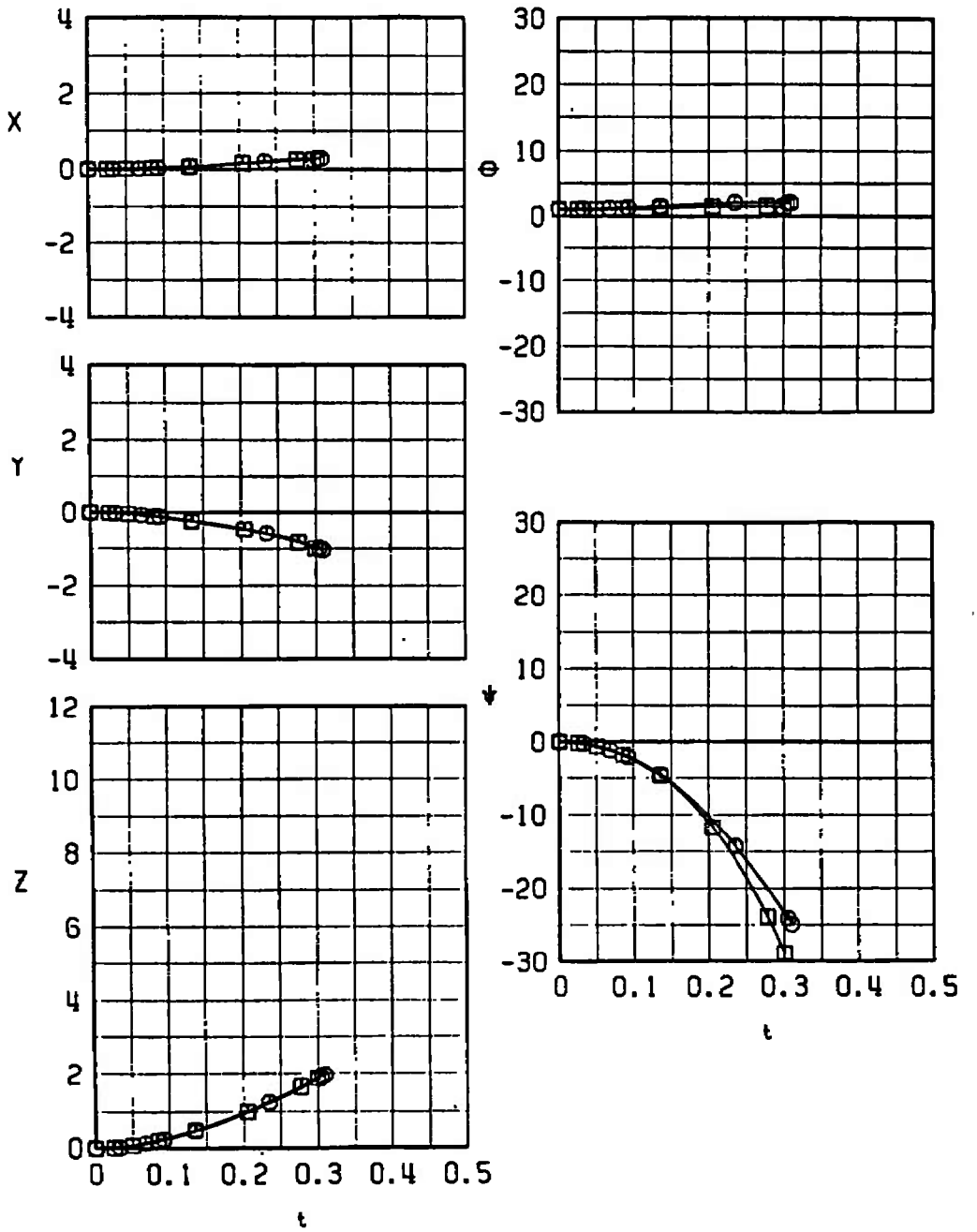

a. $M_\infty = 0.66$

Fig. 13 Effect of Shift in Moment Center on Separation Trajectories from Left Wing TER, Station 2; Fins Folded

SYM	CONF	M_∞	α	H	$\bar{\theta}$	MOMENT CENTER
□	2	0.74	1.3	5000	-45	N
○	2	0.74	1.3	5000	-45	F

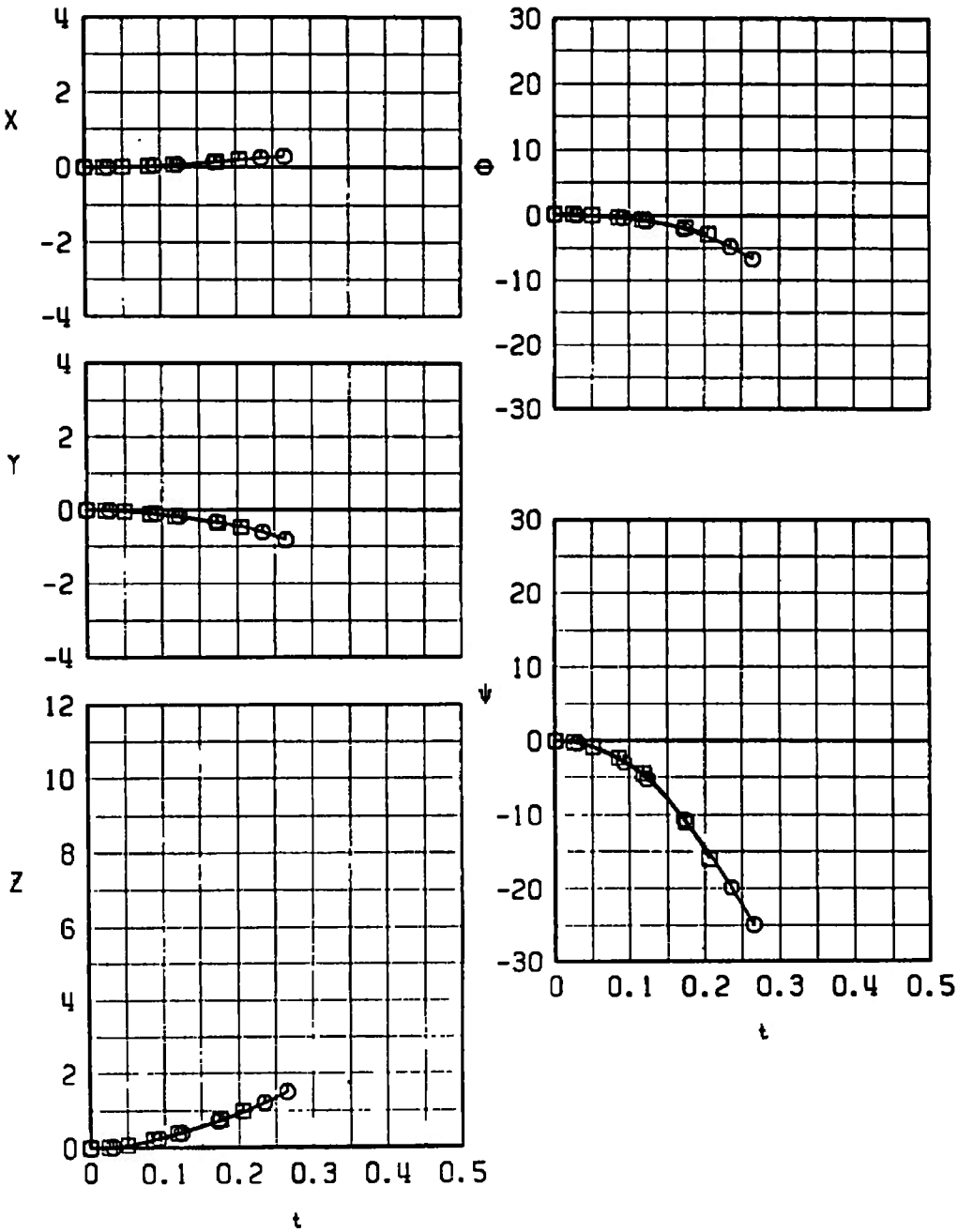

b. $M_\infty = 0.74$

Fig. 13 Continued

SYM	CONF	M_∞	α	H	$\bar{\theta}$	MOMENT CENTER
□	2	0.82	0.7	5000	-45	N
○	2	0.82	0.7	5000	-45	F

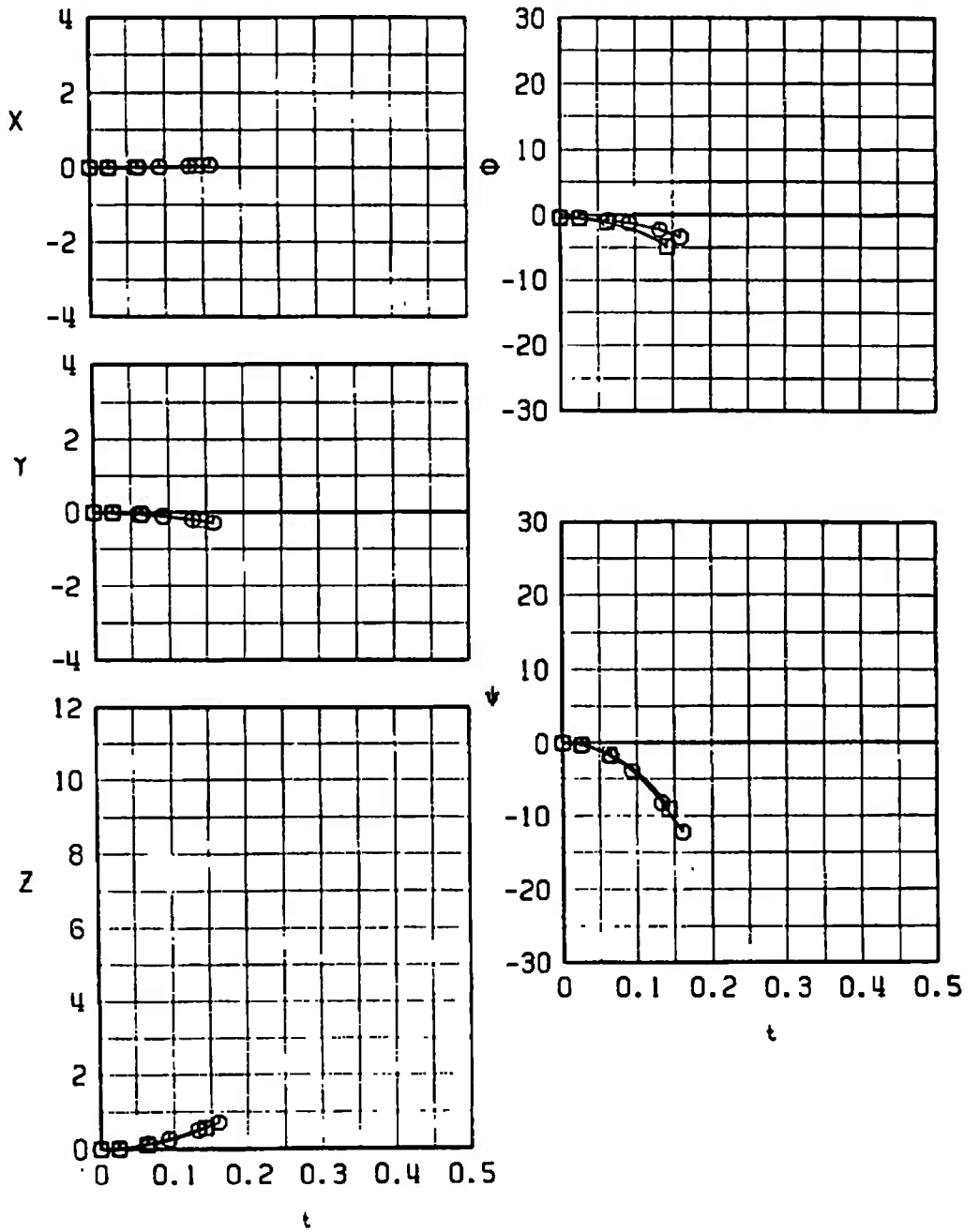

c. $M_\infty = 0.82$

Fig. 13 Continued

SYM	CONF	M_∞	α	H	$\bar{\theta}$	MOMENT CENTER
□	2	0.90	0.3	5000	-45	N
○	2	0.90	0.3	5000	-45	F

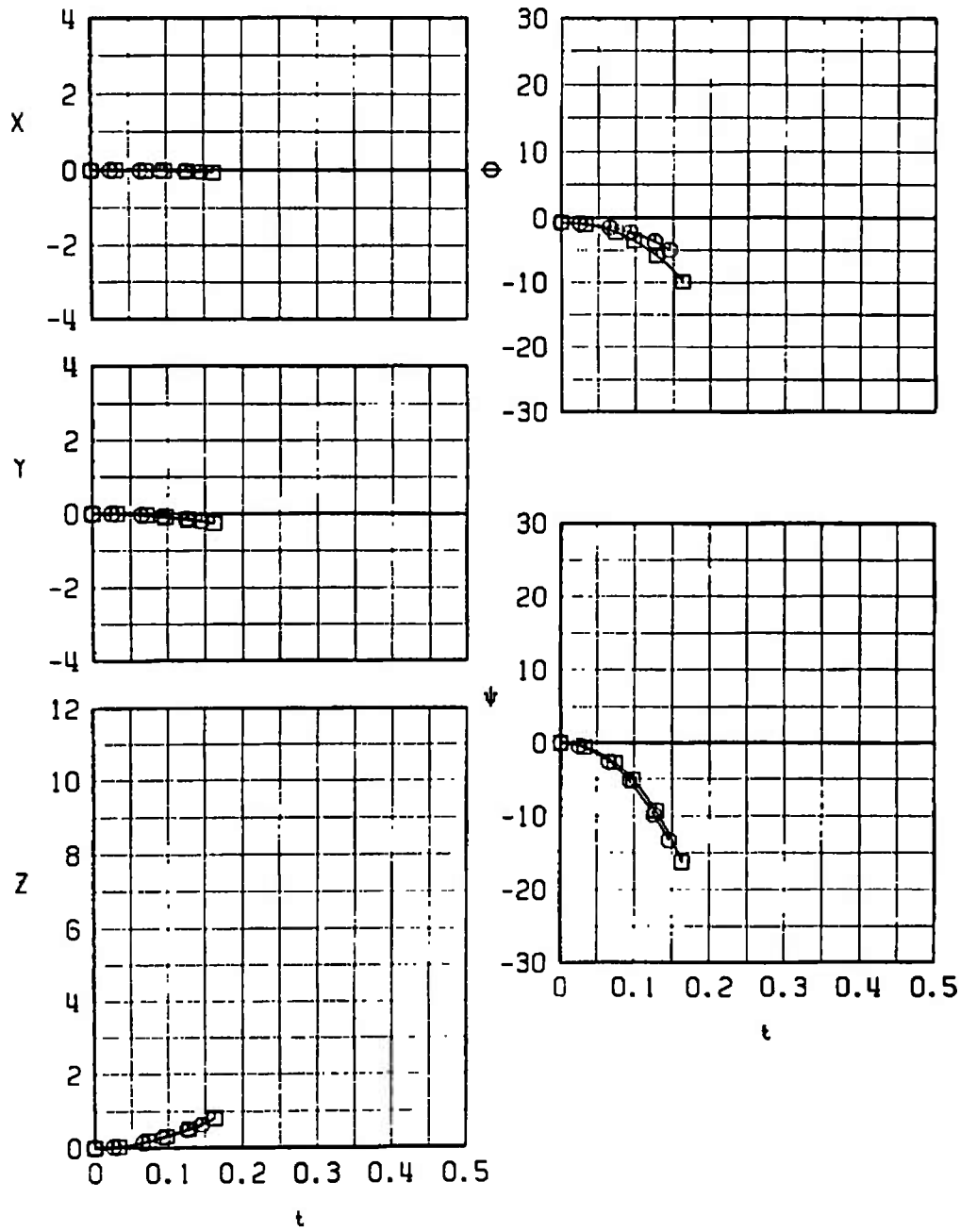

d. $M_\infty = 0.90$

Fig. 13 Concluded

SYM	CONF	M_∞	α	H	$\bar{\theta}$	MOMENT CENTER
□	1	0.74	1.3	5000	-45	N
○	1	0.82	0.7	5000	-45	N
△	1	0.90	0.3	5000	-45	N

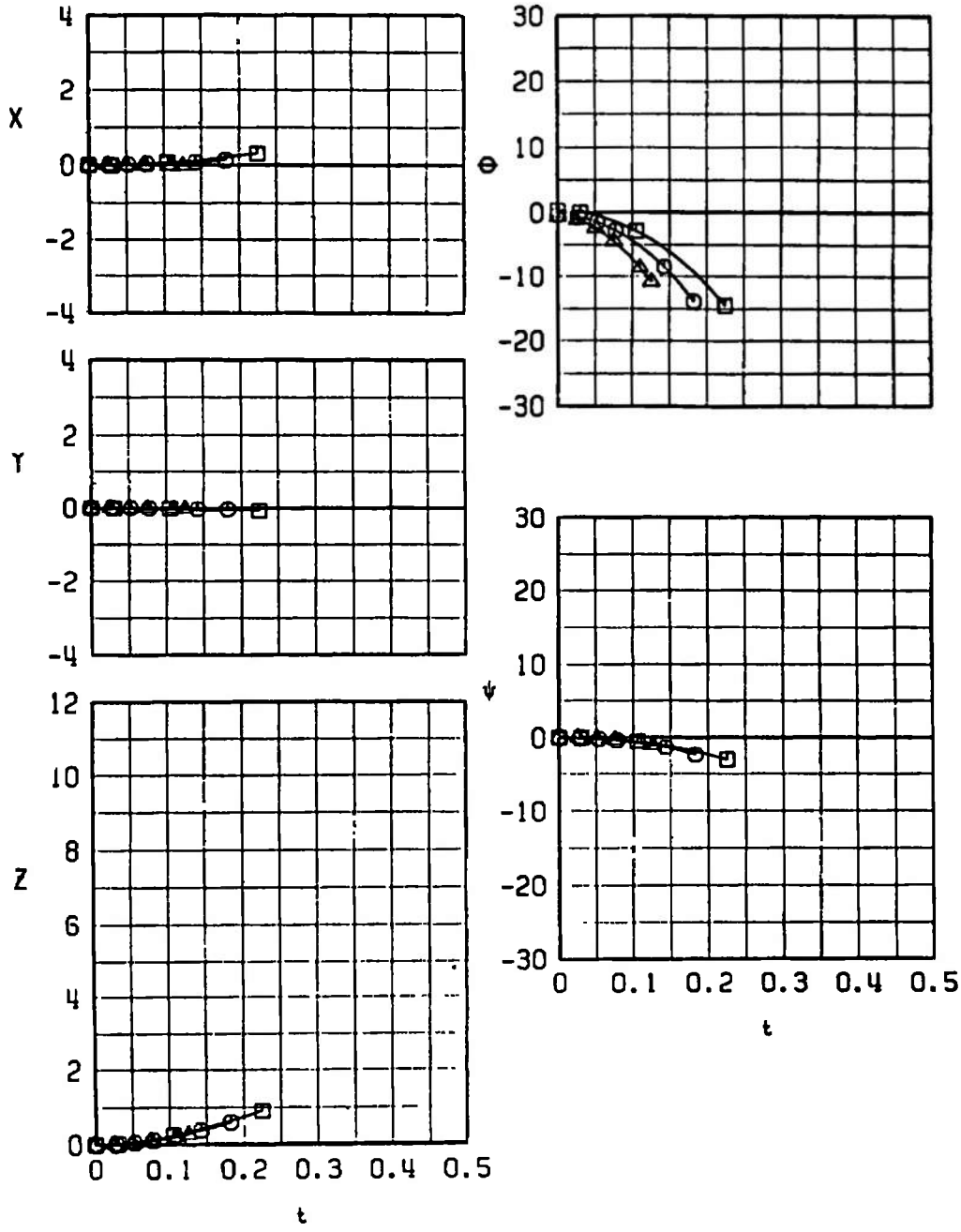

Fig. 14 Separation Trajectories from Left Wing TER, Station 1; Fins Folded

SYM	CONF	M_∞	α	H	$\bar{\theta}$	MOMENT CENTER
◁	3	0.66	2.1	.5000	0	N
□	3	0.74	1.3	5000	0	N
○	3	0.82	0.7	5000	0	N
△	3	0.90	0.3	5000	0	N

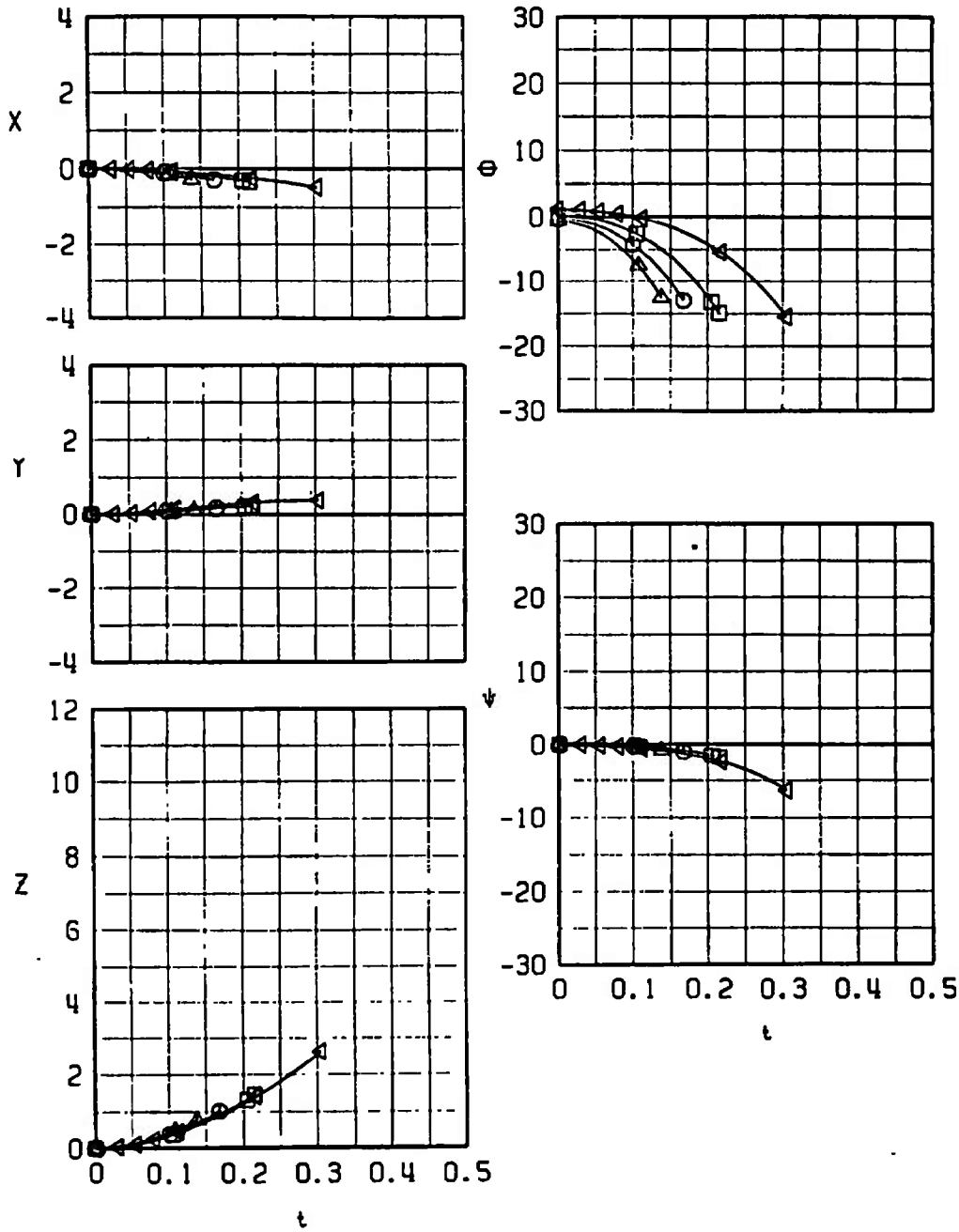

a. $\bar{\theta}$ = 0, Moment Center (N)

Fig. 15 Separation Trajectories from Left Wing TER, Station 3 (Simulated Right Wing TER, Station 2); Fins Folded

SYM	CONF	M_∞	α	H	$\bar{\theta}$	MOMENT CENTER
□	3	0.74	1.3	5000	-45	N
○	3	0.82	0.7	5000	-45	N
△	3	0.90	0.3	5000	-45	N

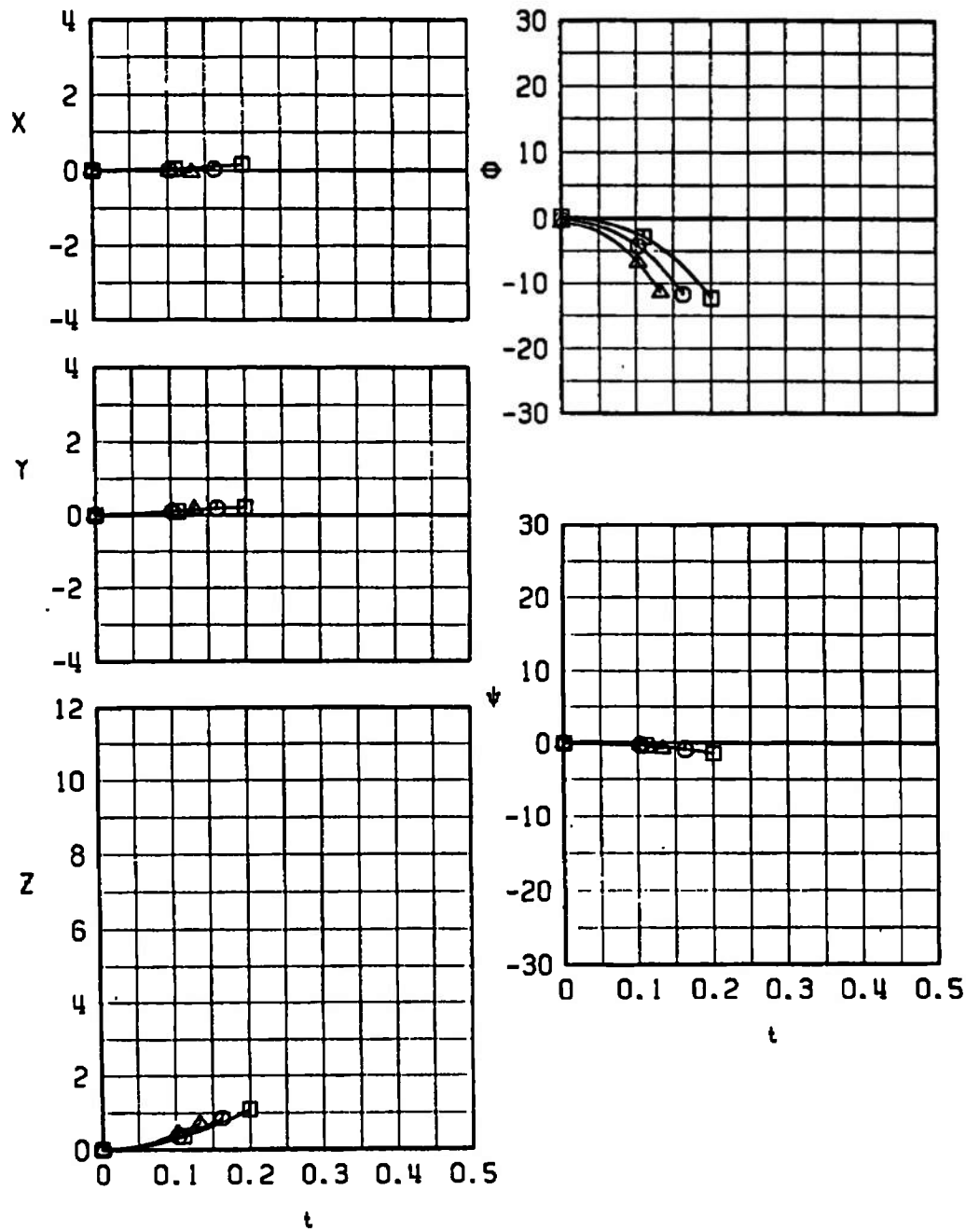

b. $\bar{\theta}$ = -45, Moment Center (N)

Fig. 15 Continued

SYM	CONF	M_∞	α	H	$\bar{\theta}$	MOMENT CENTER
⊙	3	0.82	0.7	5000	-45	F
△	3	0.90	0.3	5000	-45	F

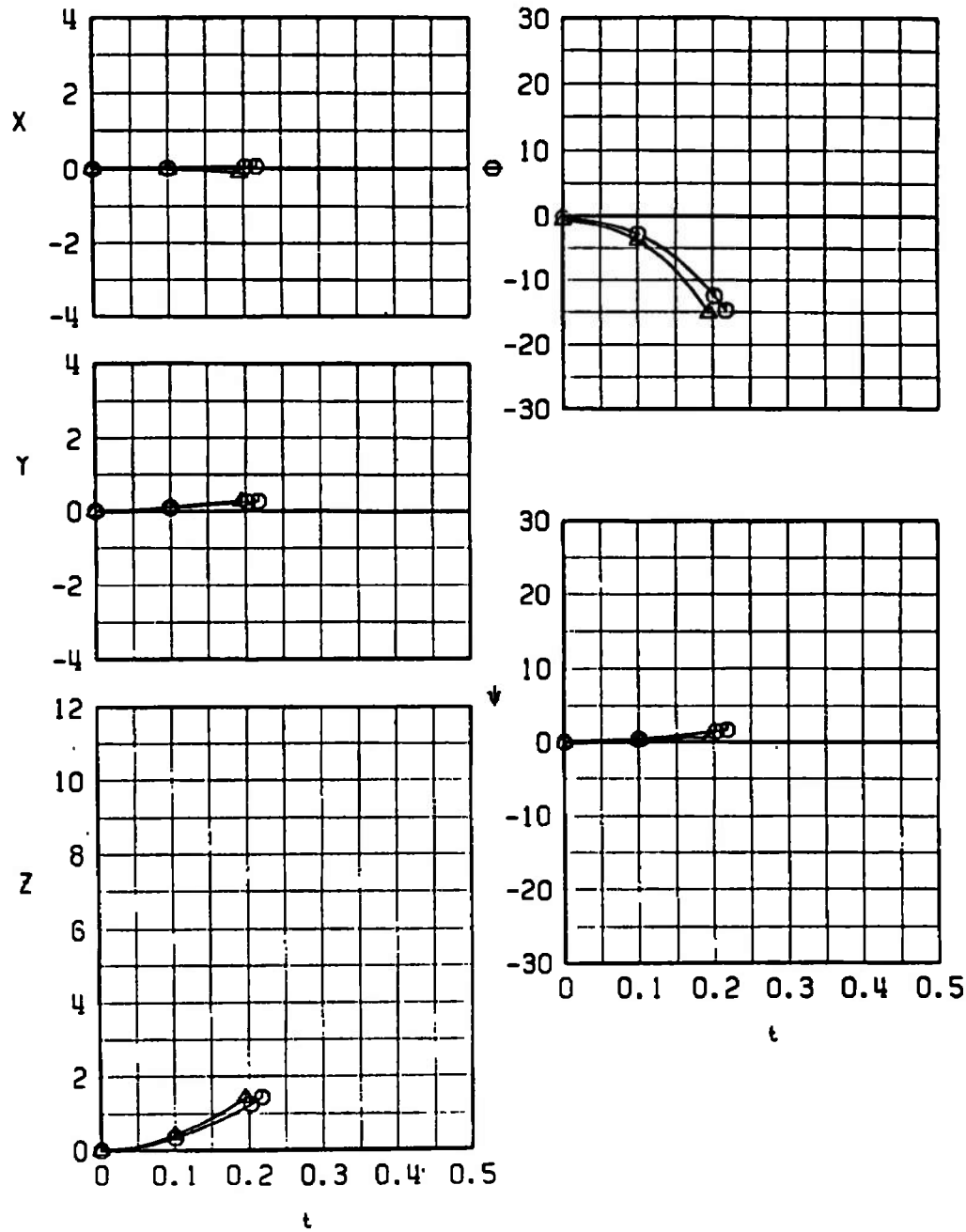

c. $\bar{\theta}$ = -45, Moment Center (F)

Fig. 15 Concluded

SYM	CONF	M_∞	α	H	$\bar{\theta}$	MOMENT CENTER
◁	4	0.66	2.1	5000	0	N
□	4	0.74	1.3	5000	0	N
○	4	0.82	0.7	5000	0	N
△	4	0.90	0.3	5000	0	N

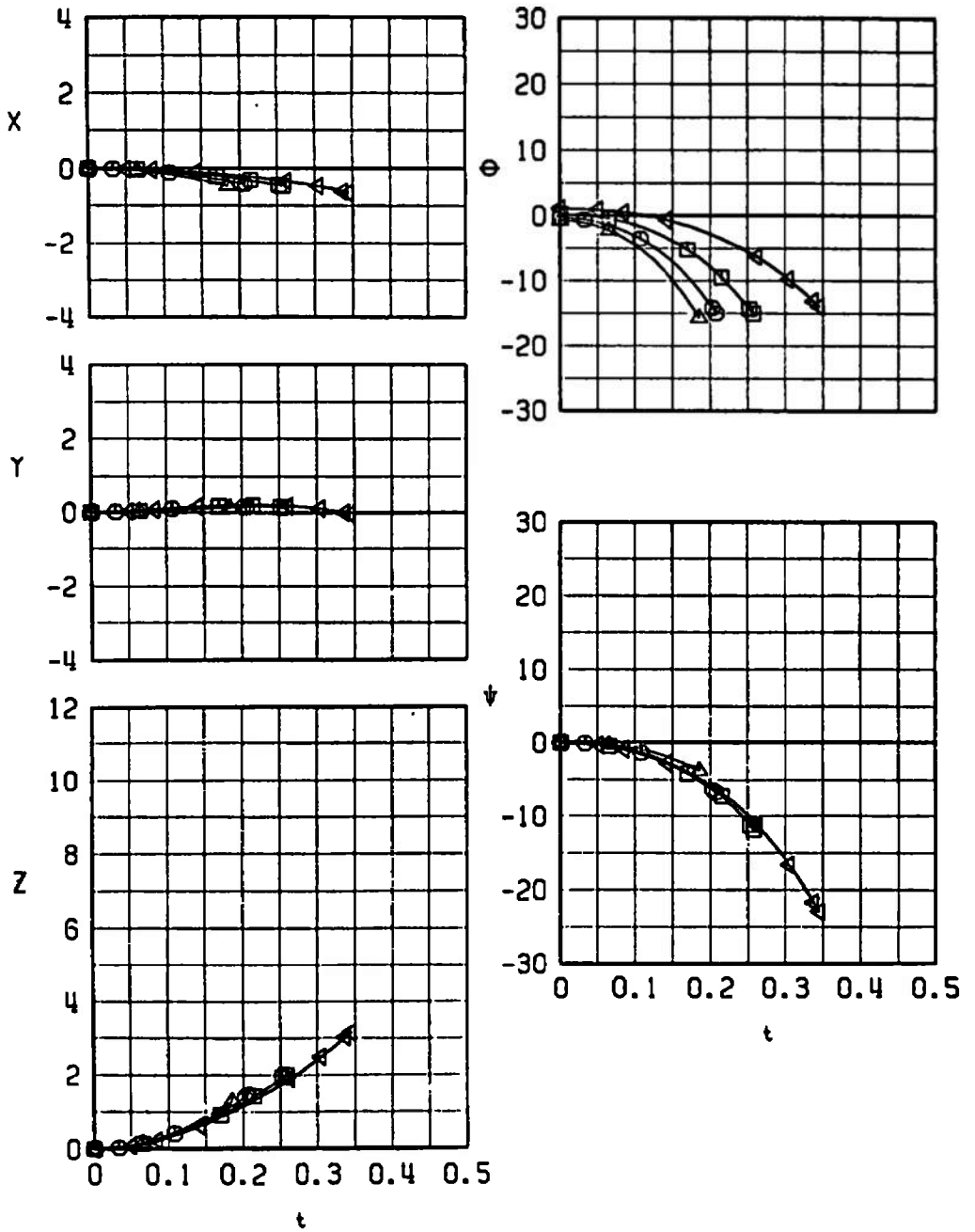

a. $\bar{\theta}$ = 0, Moment Center (N)

Fig. 16 Separation Trajectories from Left Wing TER, Station 3; Fins Folded

SYM	CONF	M_∞	α	H	$\bar{\theta}$	MOMENT CENTER
□	4	0.74	1.3	5000	-45	N
○	4	0.82	0.7	5000	-45	N
△	4	0.90	0.3	5000	-45	N

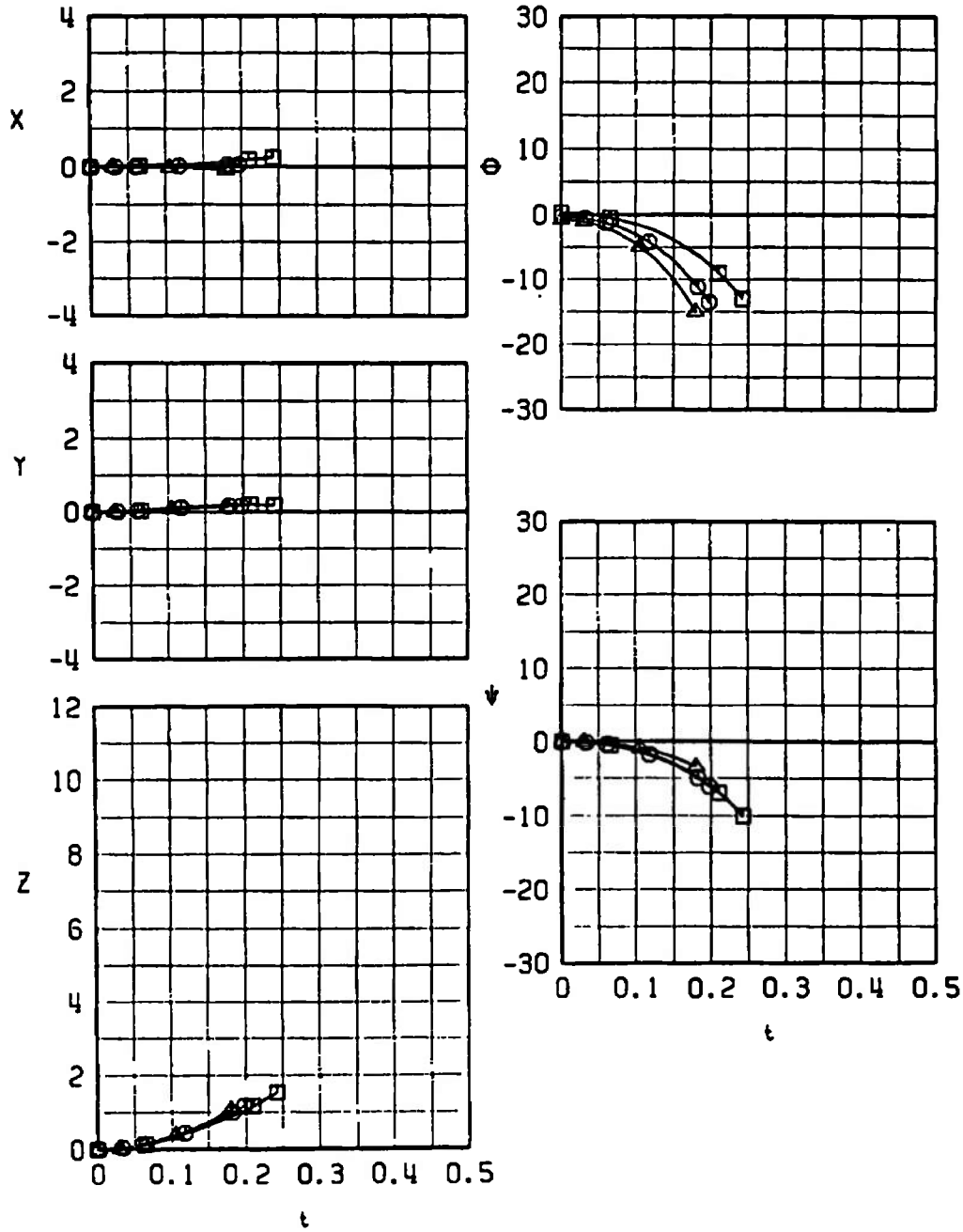

b. $\bar{\theta}$ = -45, Moment Center (N)
Fig. 16 Continued

SYM	CONF	M_∞	α	H	$\bar{\theta}$	MOMENT CENTER
□	4	0.74	1.3	5000	-45	F
○	4	0.82	0.7	5000	-45	F
△	4	0.90	0.3	5000	-45	F

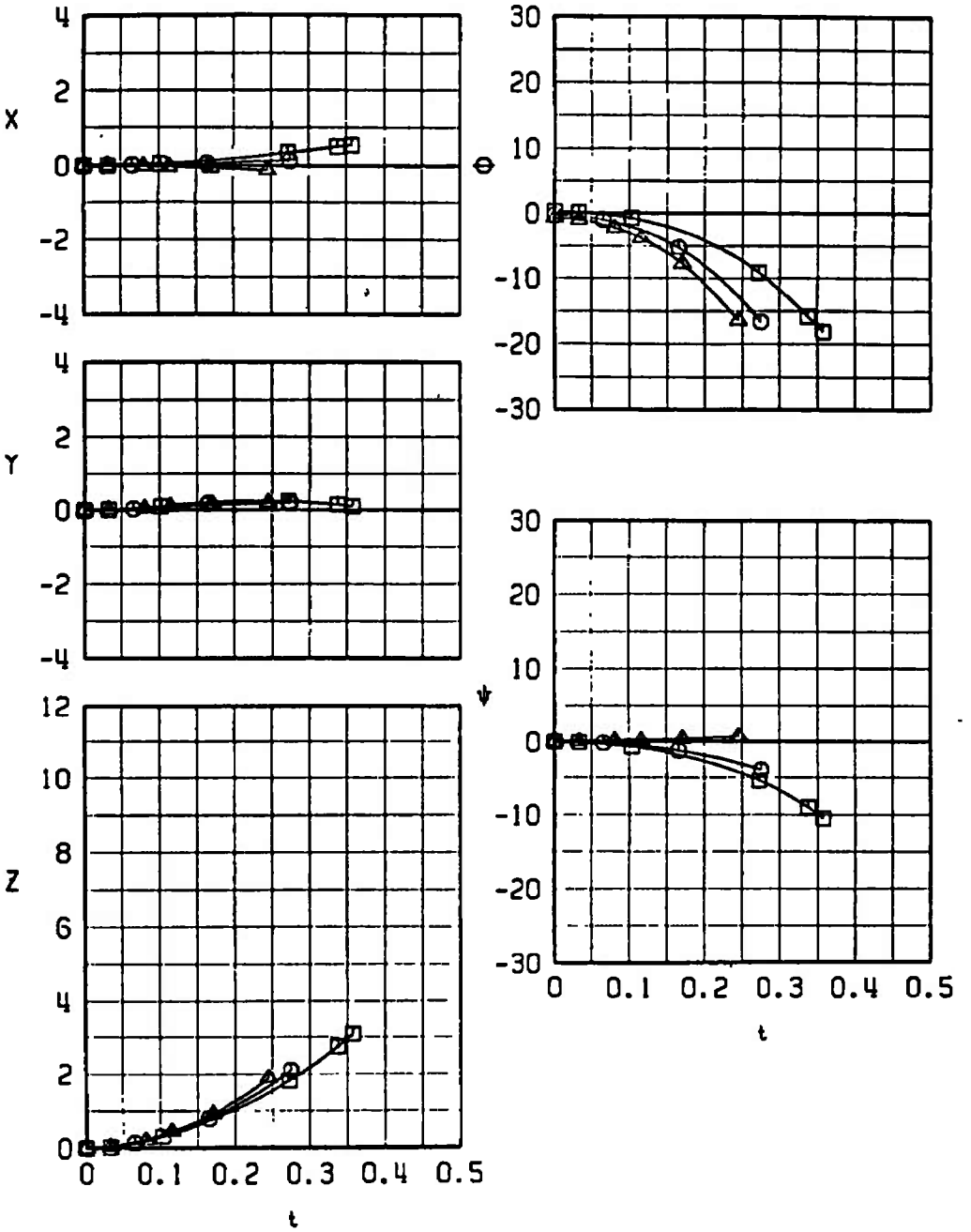

c. $\bar{\theta}$ = -45, Moment Center (F)

Fig. 16 Concluded

SYM	CONF	M_∞	α	H	$\bar{\theta}$	MOMENT CENTER
◁	5	0.66	2.1	5000	0	N
□	5	0.74	1.3	5000	0	N
○	5	0.82	0.7	5000	0	N
△	5	0.90	0.3	5000	0	N

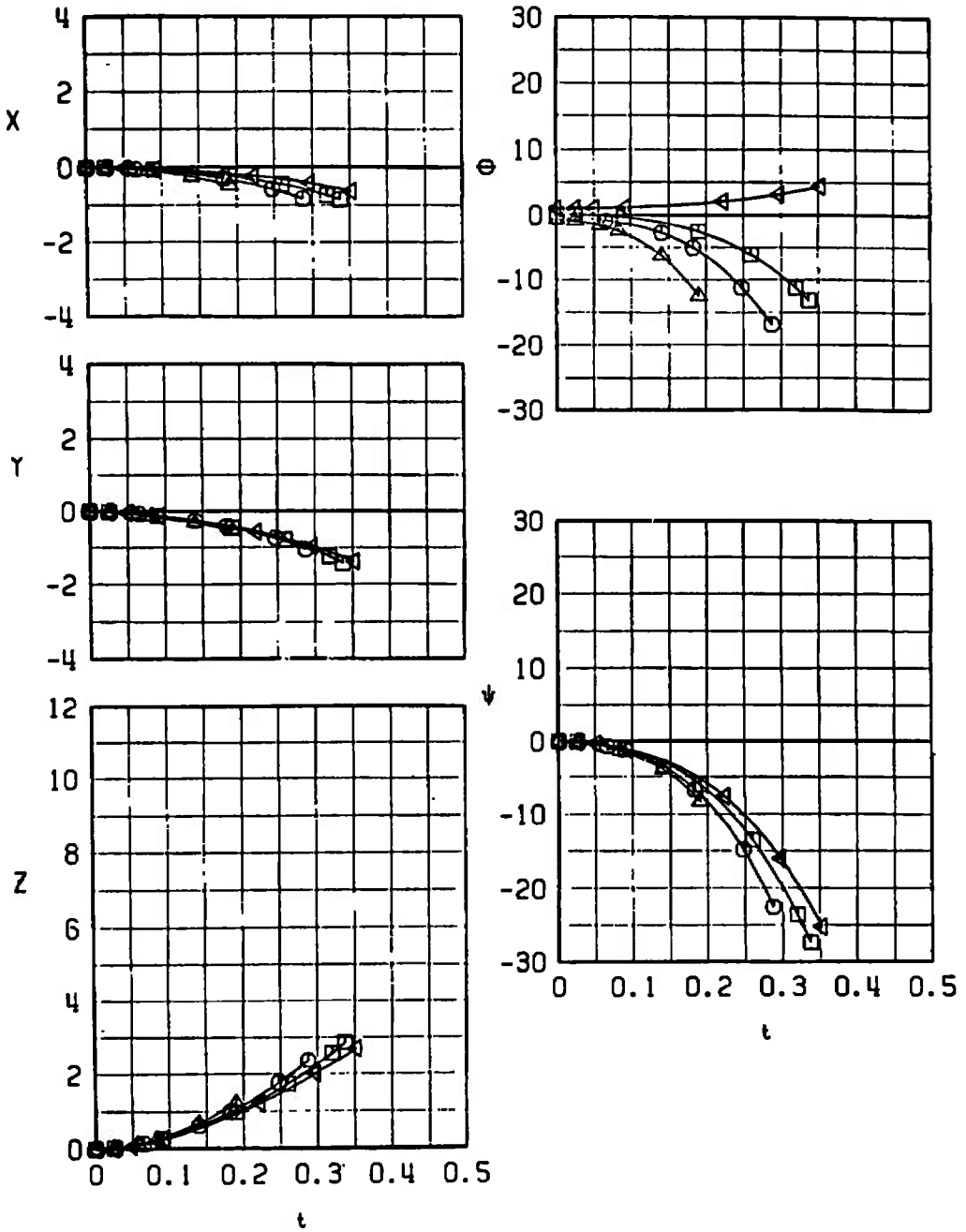

a. $\bar{\theta}$ = 0, Moment Center (N)

Fig. 17 Separation Trajectories from Left Wing TER, Station 2 (Simulated Right Wing TER, Station 3); Fins Folded

SYM	CONF	M_∞	α	H	$\bar{\theta}$	MOMENT CENTER
⊡	5	0.74	1.3	5000	-45	N
⊙	5	0.82	0.7	5000	-45	N
△	5	0.90	0.3	5000	-45	N

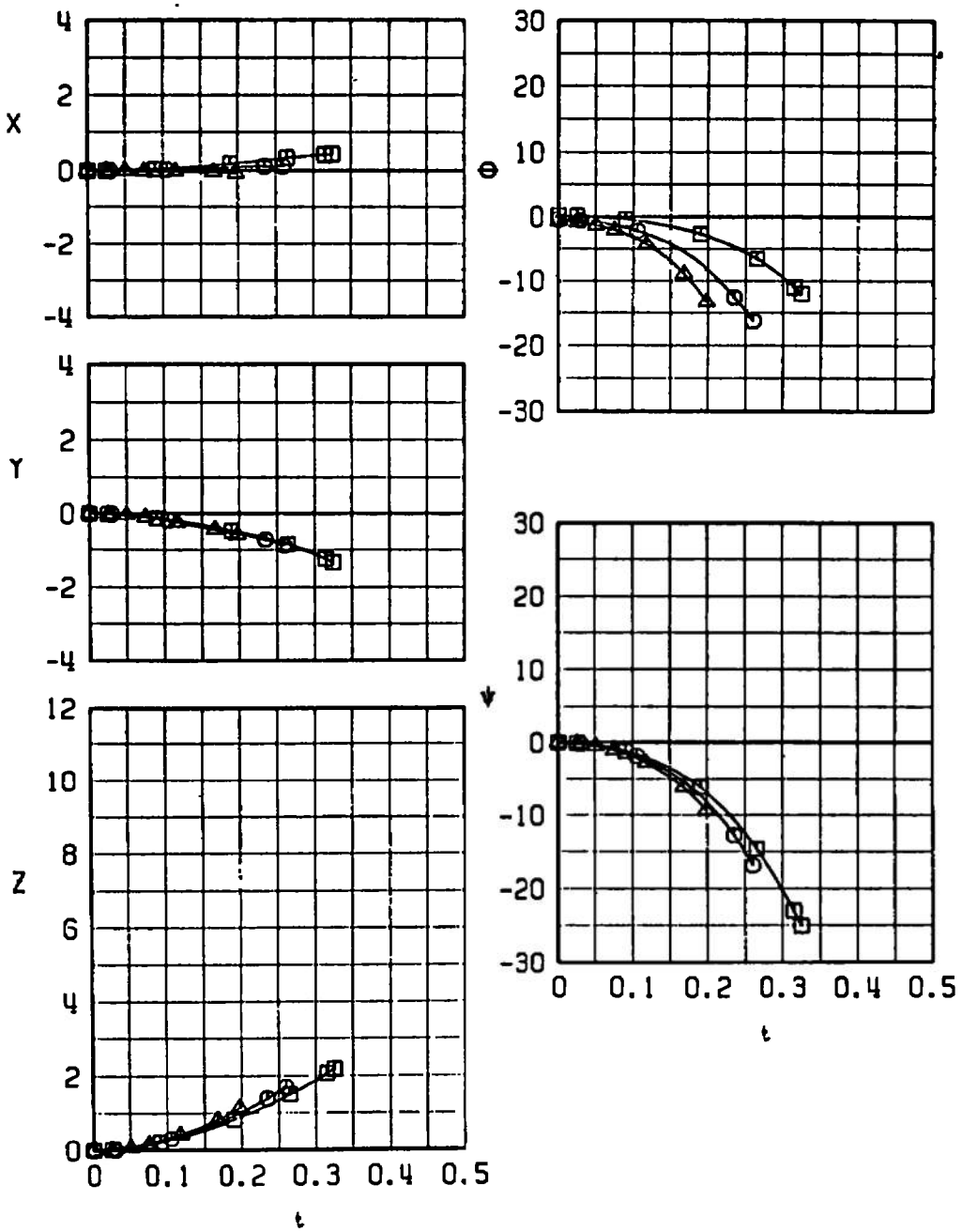

b. $\bar{\theta}$ = -45, Moment Center (N)
Fig. 17 Continued

SYM	CONF	M_∞	α	H	$\bar{\theta}$	MOMENT CENTER
□	5	0.74	1.3	5000	-45	F
○	5	0.82	0.7	5000	-45	F
△	5	0.90	0.3	5000	-45	F

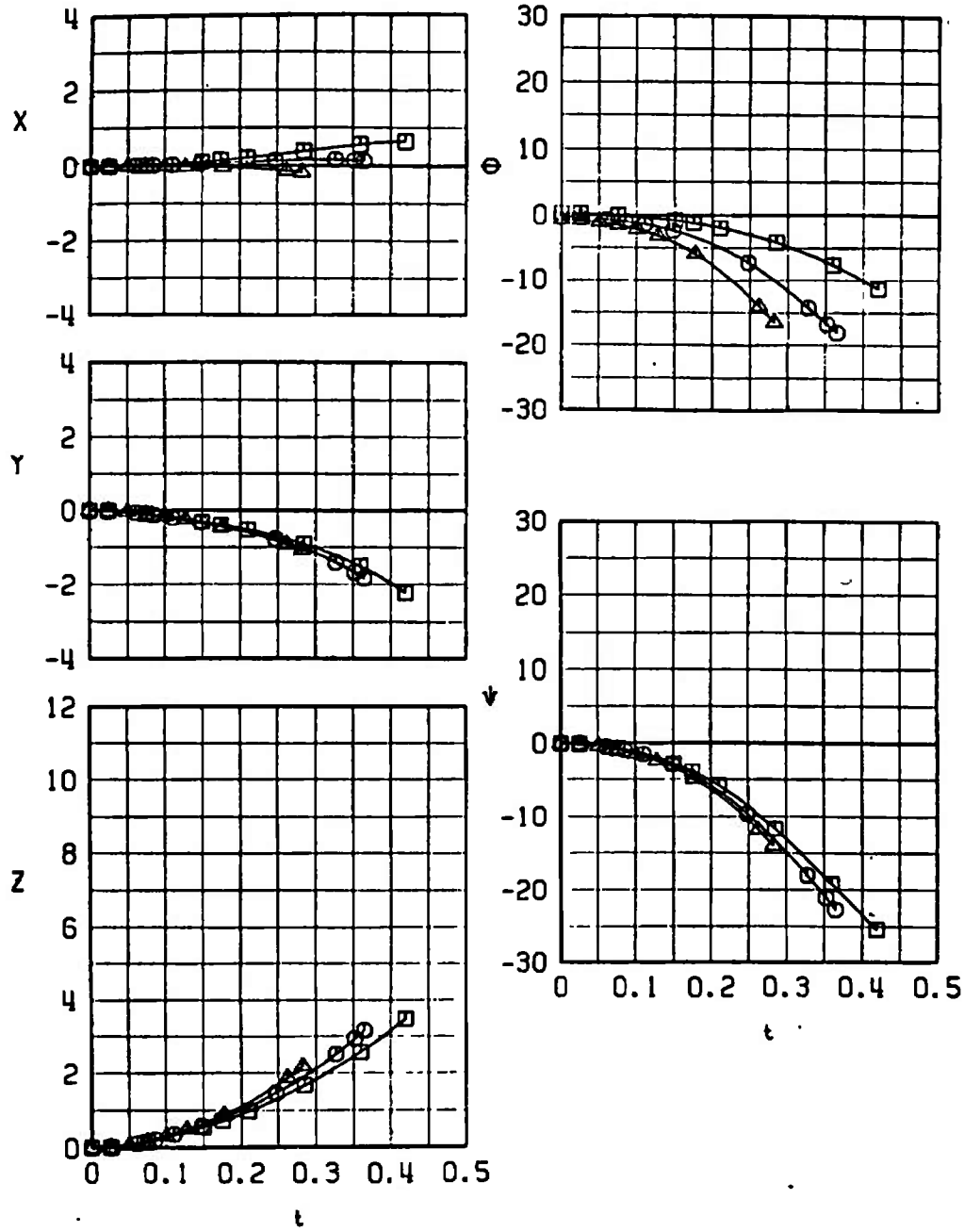

c. $\bar{\theta}$ = -45, Moment Center (F)

Fig. 17 Concluded

SYM	CONF	M_∞	α	H	$\bar{\theta}$	MOMENT CENTER
◁	7	0.66	2.1	5000	0	N
□	7	0.74	1.3	5000	0	N
○	7	0.82	0.7	5000	0	N
△	7	0.90	0.3	5000	0	N

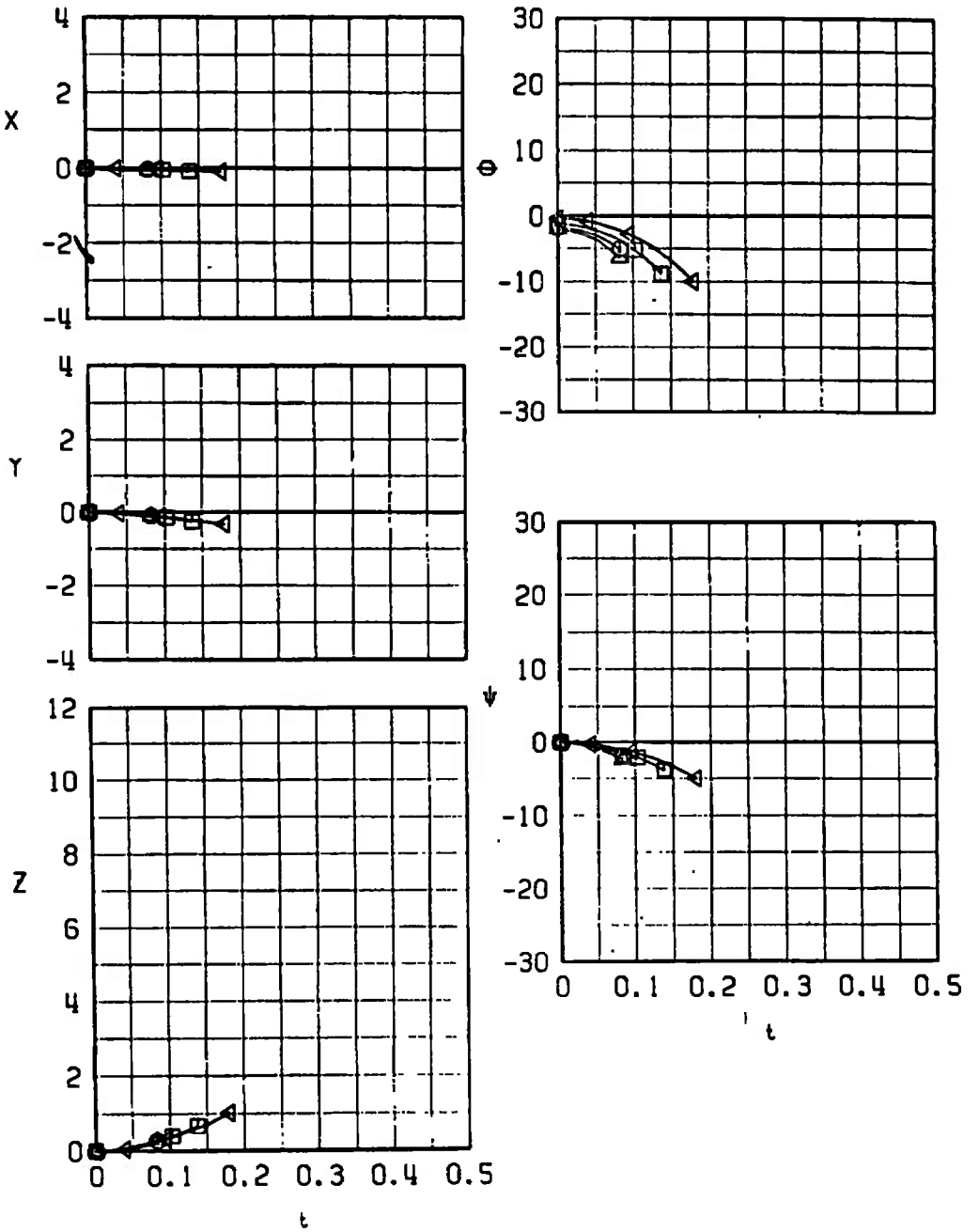

a. $\bar{\theta}$ = 0, Moment Center (N)

Fig. 18 Separation Trajectories from Centerline MER, Station 3; Fins Folded

SYM	CONF	M_∞	α	H	$\bar{\theta}$	MOMENT CENTER
□	7	0.74	1.3	5000	-45	N
○	7	0.82	0.7	5000	-45	N
△	7	0.90	0.3	5000	-45	N

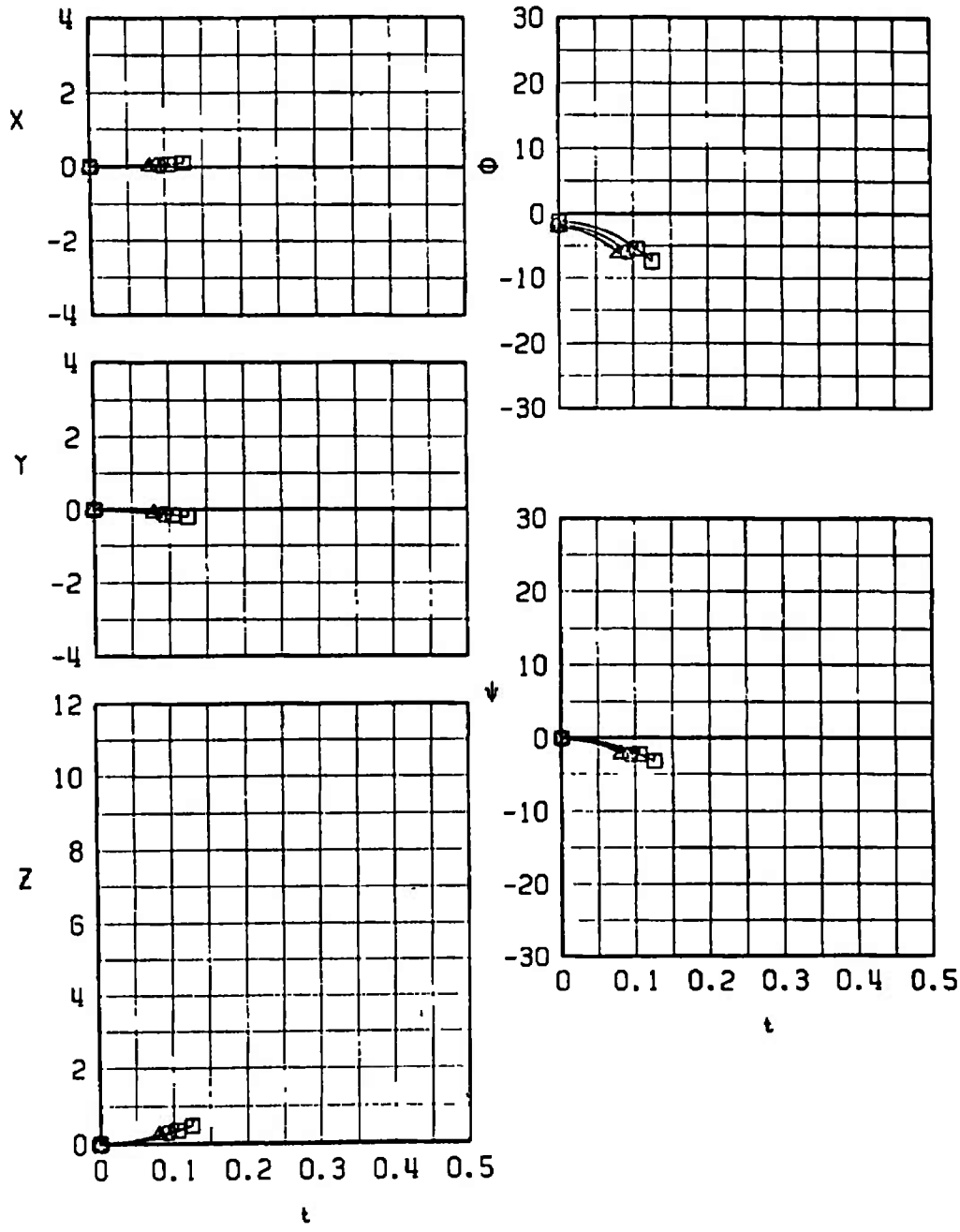

b. $\bar{\theta}$ = -45, Moment Center (N)
Fig. 18 Continued

SYM	CONF	M_∞	α	H	$\bar{\theta}$	MOMENT CENTER
□	7	0.74	1.3	5000	-45	F
○	7	0.82	0.7	5000	-45	F
△	7	0.90	0.3	5000	-45	F

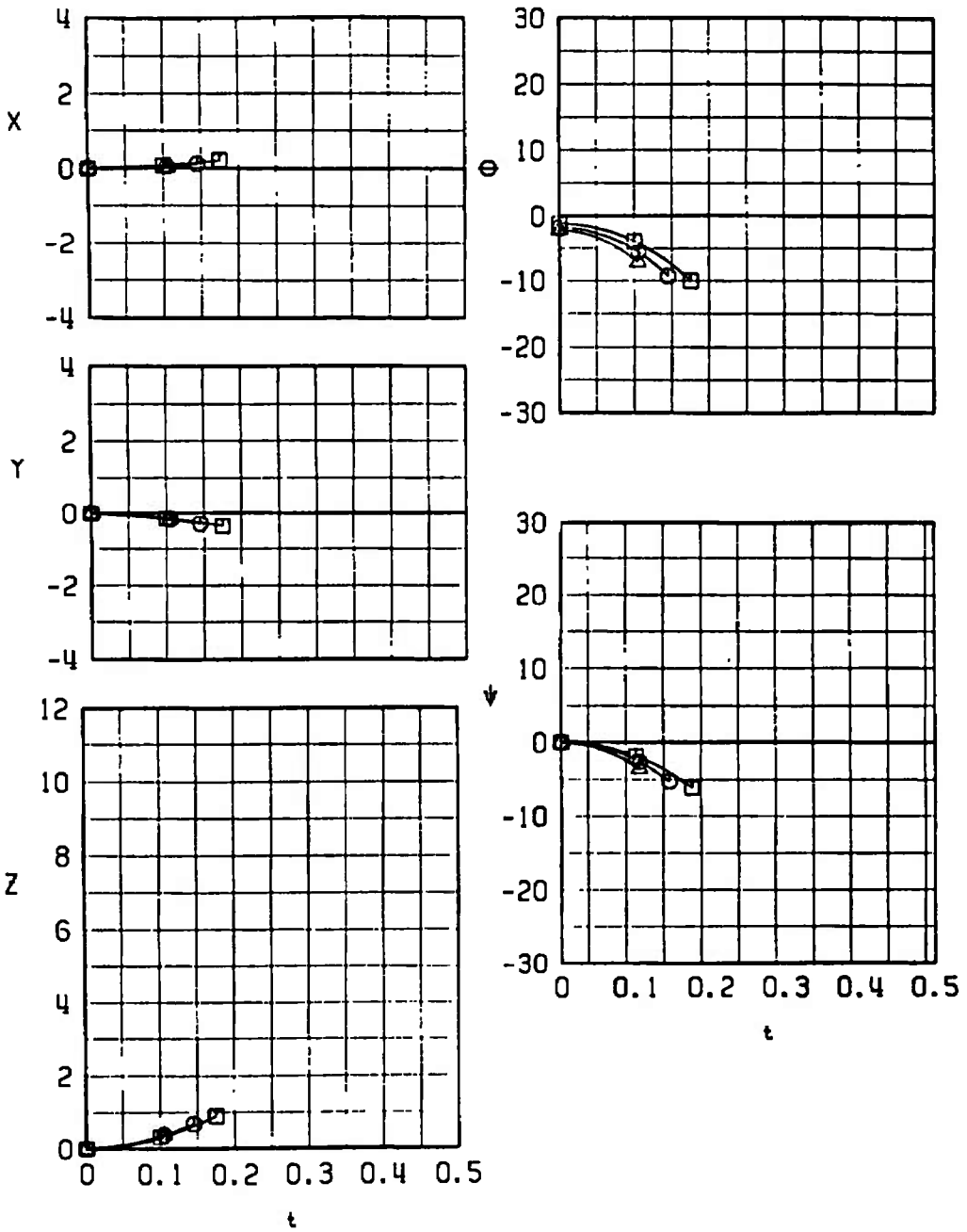

c. $\bar{\theta}$ = -45, Moment Center (F)

Fig. 18 Concluded

SYM	CONF	M_∞	α	H	$\bar{\theta}$	MOMENT CENTER
◁	8	0.66	2.1	5000	0	N
□	8	0.74	1.3	5000	0	N
○	8	0.82	0.7	5000	0	N
△	8	0.90	0.3	5000	0	N

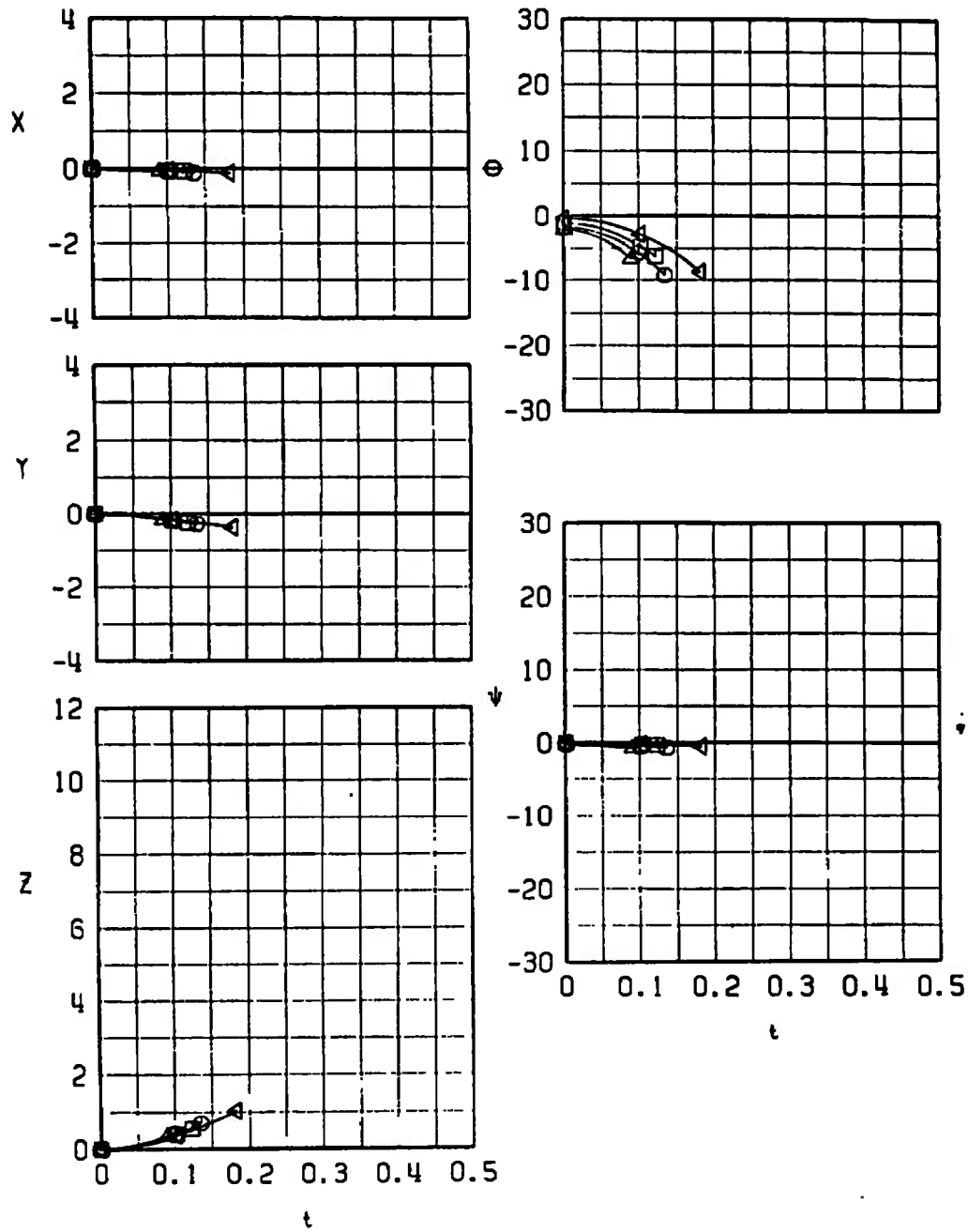

a. $\bar{\theta}$ = 0, Moment Center (N)

Fig. 19 Separation Trajectories from Centerline MER, Station 3 (Simulated Centerline MER, Station 5); Fins Folded

SYM	CONF	M_∞	α	H	$\bar{\theta}$	MOMENT CENTER
⊡	8	0.74	1.3	5000	-45	N
⊙	8	0.82	0.7	5000	-45	N
△	8	0.90	0.3	5000	-45	N

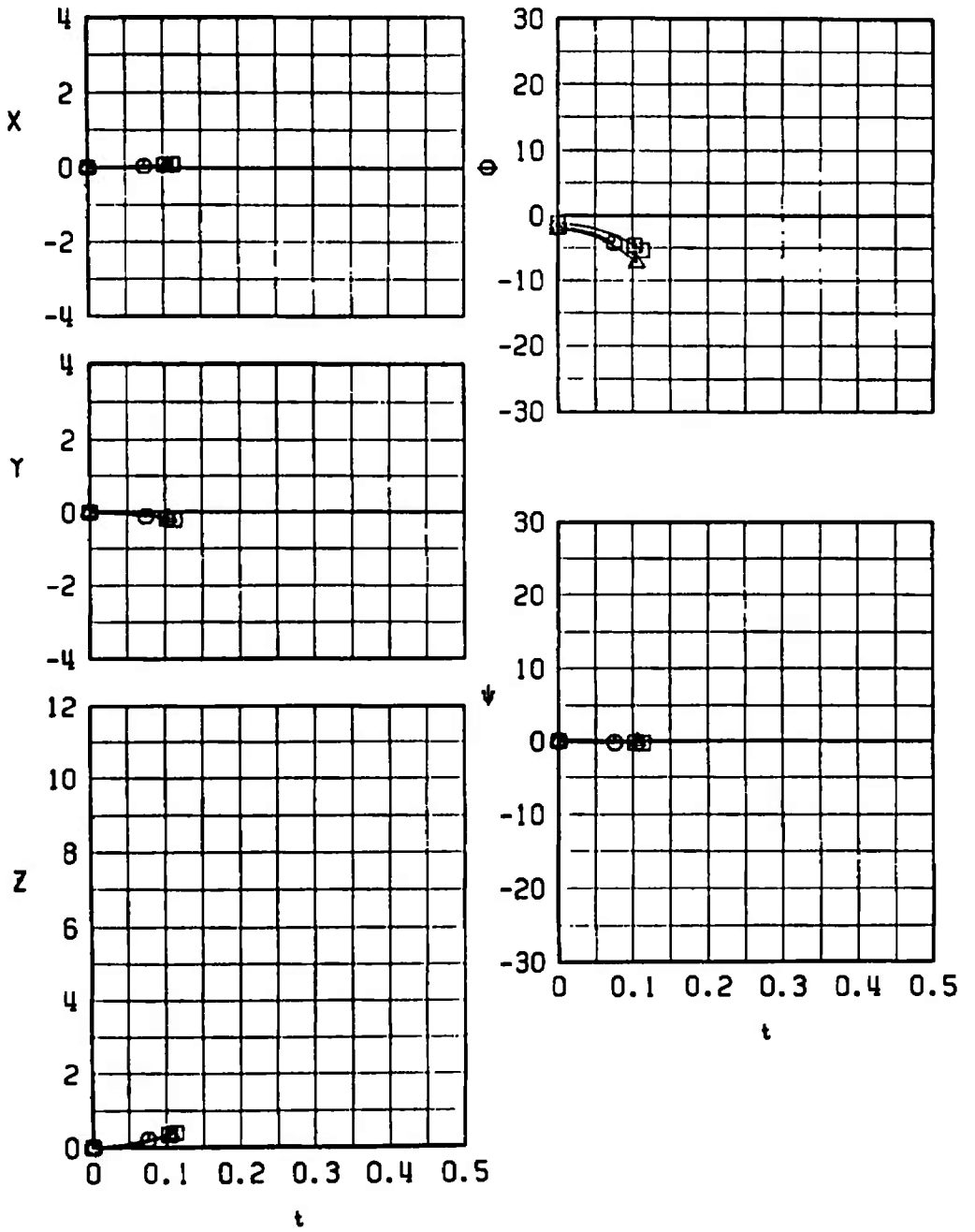

b. $\bar{\theta}$ = -45, Moment Center (N)

Fig. 19 Continued

SYM	CONF	M_∞	α	H	$\bar{\theta}$	MOMENT CENTER
□	8	0.74	1.3	5000	-45	F
○	8	0.82	0.7	5000	-45	F
△	8	0.90	0.3	5000	-45	F

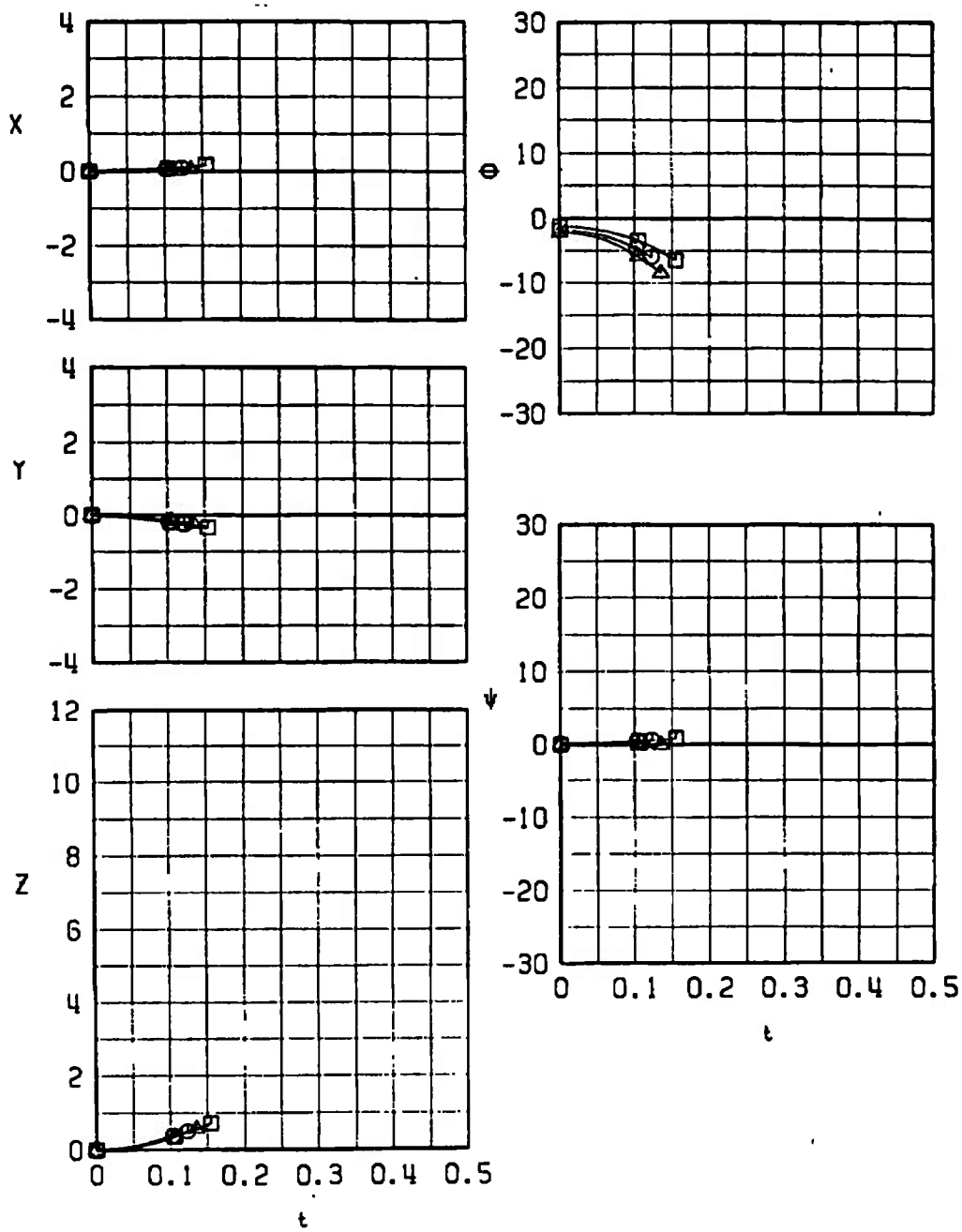

c. $\bar{\theta}$ = -45, Moment Center (F)

Fig. 19 Concluded

FINS	SYM	CONF	M_∞	α	H	$\bar{\theta}$	MOMENT CENTER
FOLDED	□	4	0.66	2.1	5000	-30	N
OPEN	△	4	0.66	2.1	5000	-30	N

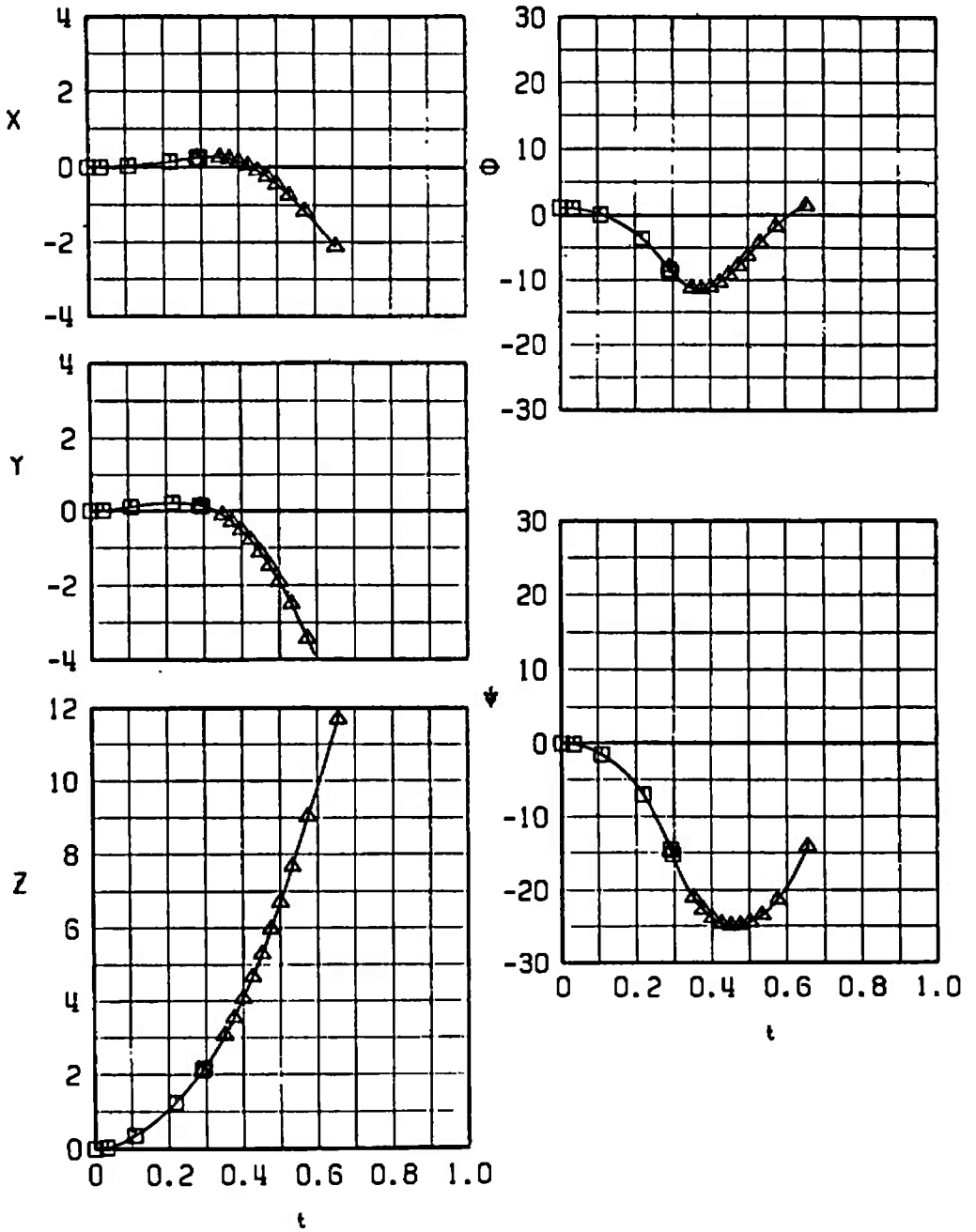

a. Load Configuration 4

Fig. 20 Effect of Open Fins on the Separation Trajectories for Selected Launch Conditions

FINS	SYM	CONF	M_∞	α	H	$\bar{\theta}$	MOMENT CENTER
FOLDED	□	5	0.66	2.1	5000	0	N
OPEN	△	5	0.66	2.1	5000	0	N
FOLDED	○	5	0.82	0.7	5000	-45	F
OPEN	◁	5	0.82	0.7	5000	-45	F

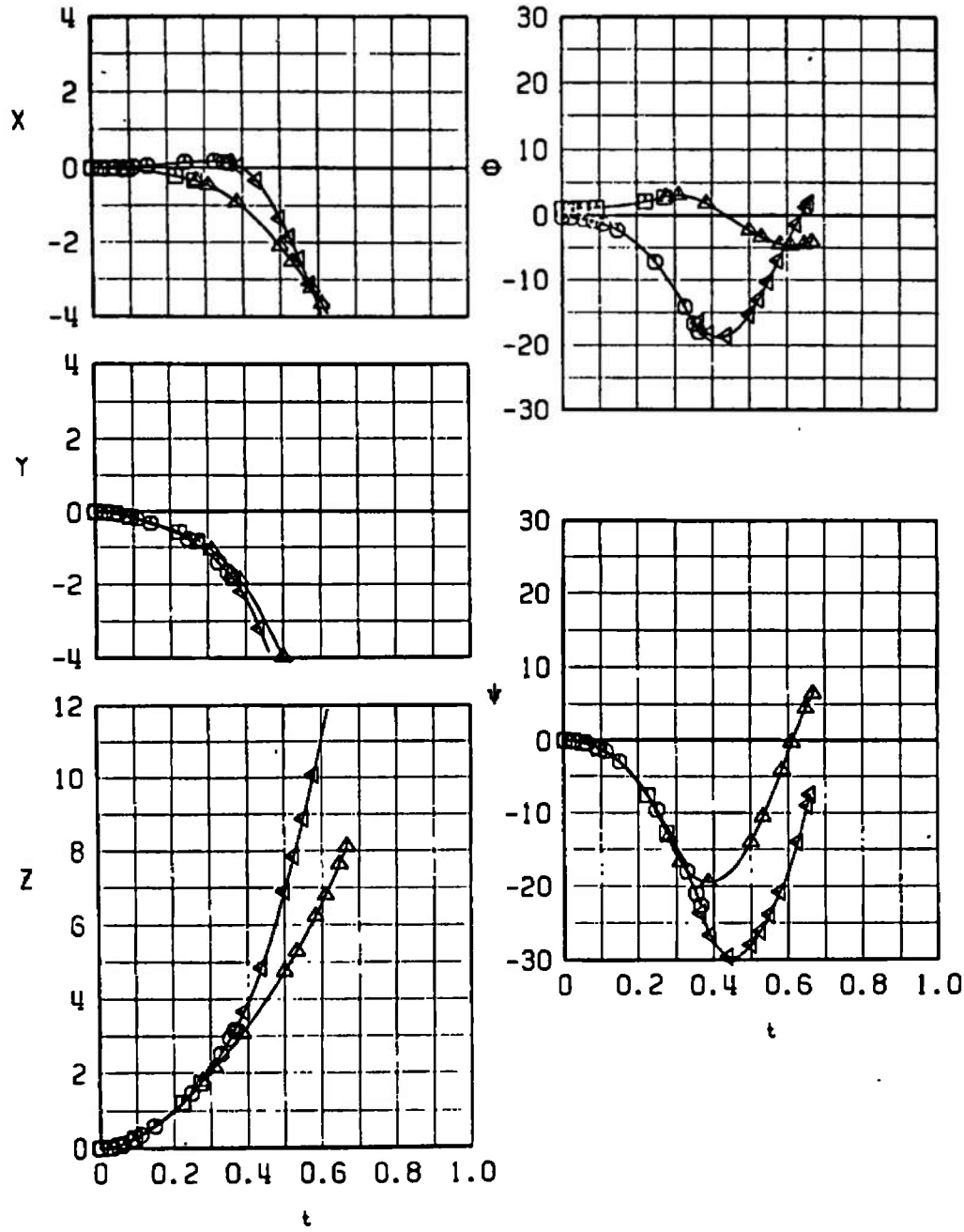

b. Load Configuration 5
Fig. 20 Continued

FINS	SYM	CONF	M_∞	α	H	$\bar{\theta}$	MOMENT CENTER
FOLDED	□	6	0.74	1.3	5000	0	N
OPEN	△	6	0.74	1.3	5000	0	N

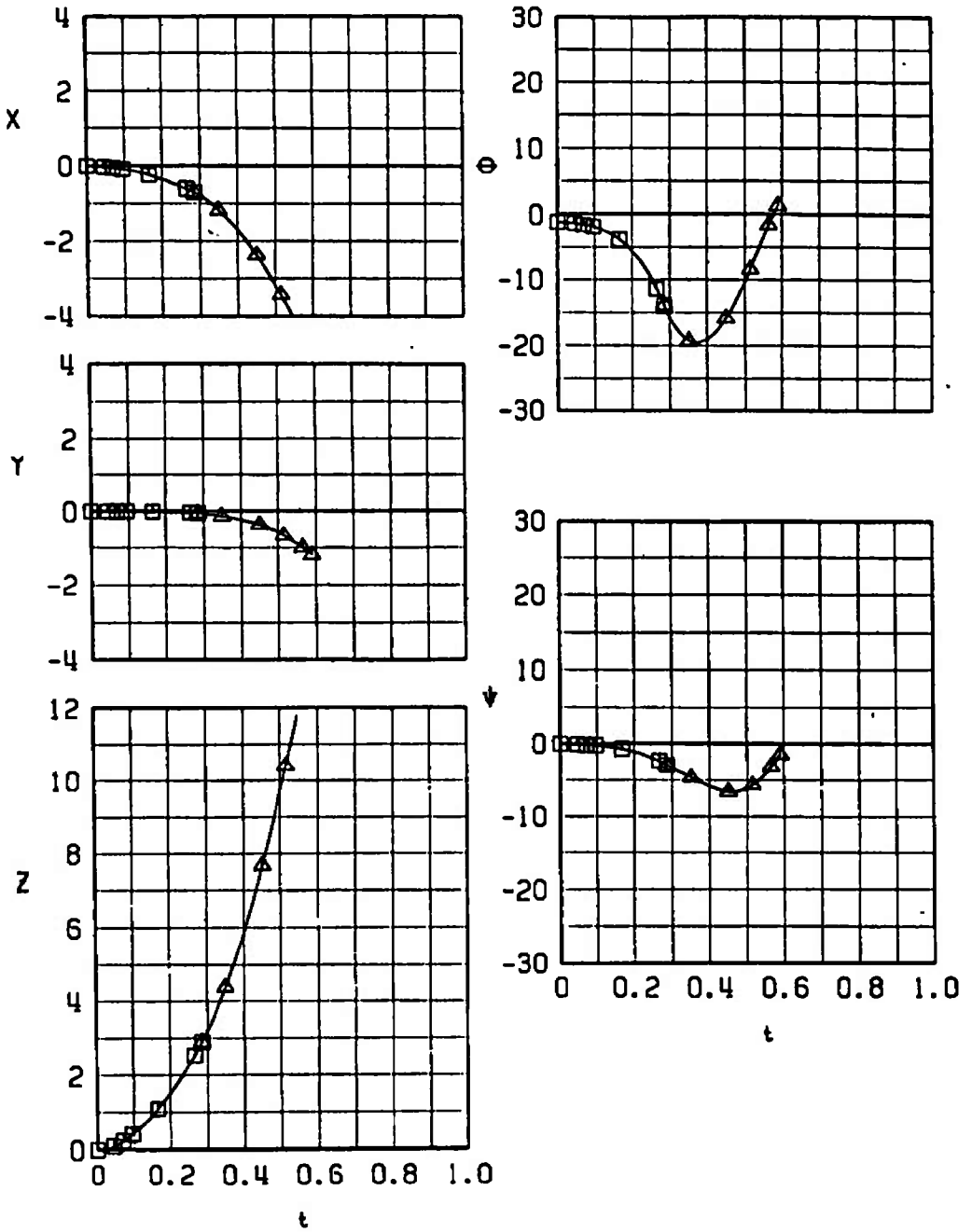

c. Load Configuration 6
Fig. 20 Concluded

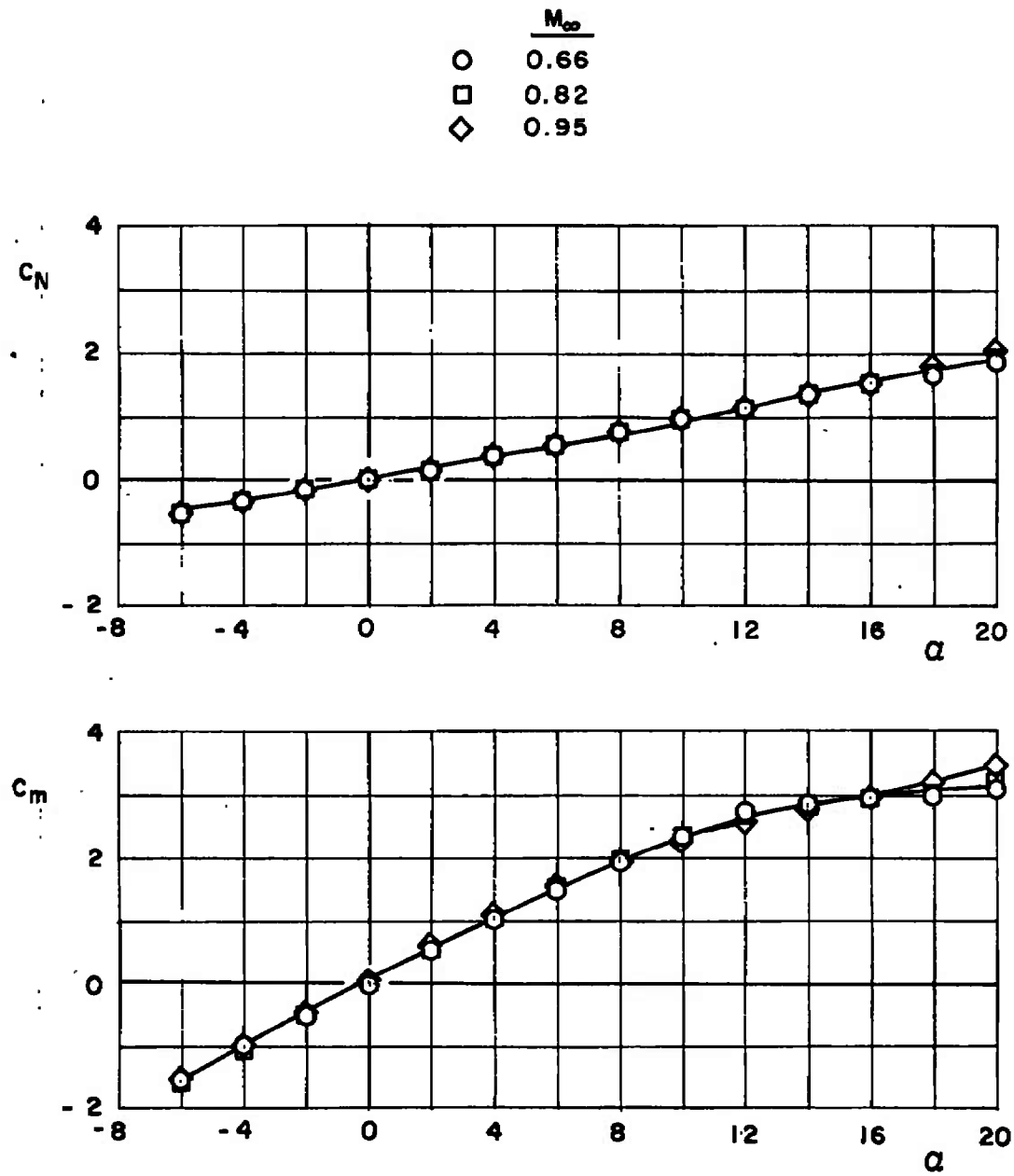

Fig. 21 Free-Stream Static Stability Data for the SUU-51 (LGDM) with Fins Folded

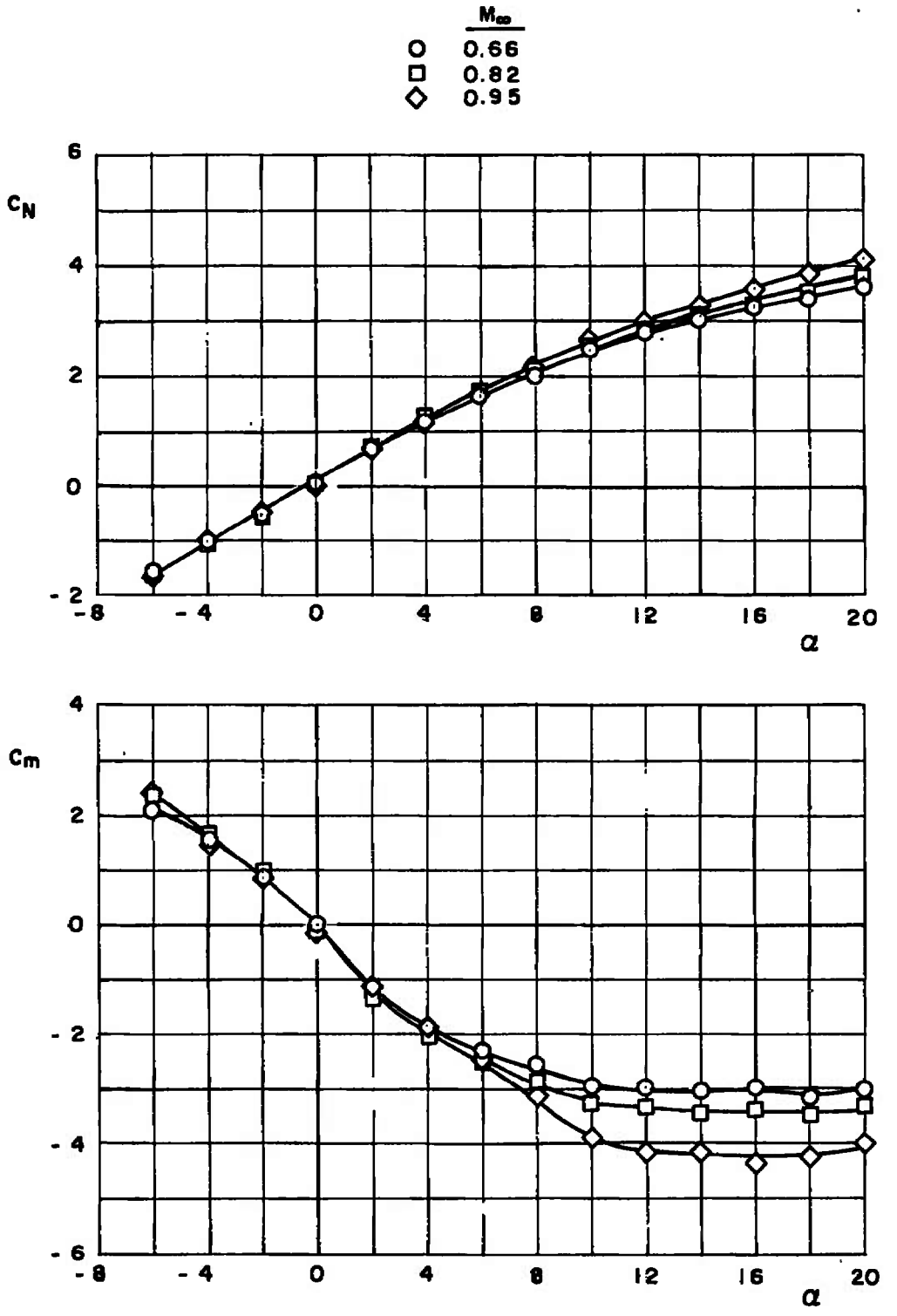

Fig. 22 Free-Stream Static Stability Data for the SUU-51 (LGDM) with Fins Open

TABLE I
FULL-SCALE STORE PARAMETERS USED IN THE TRAJECTORY CALCULATIONS

Parameter	Folded Fin Configuration	Open Fin Configuration
Mass, $\bar{m}$, slugs	31.056	31.056
Center-of-gravity location, X_{cg}, ft	6.583	6.598
Location of ejector force, X_L, ft	-0.142	
Ejector stroke length, Z_E, ft	0.2552	
Distance of the store cg above the store axial centerline, ft	0.0175	0.0175
Store reference area, S, ft^2	1.3963	1.3963
Store reference diameter, b, ft	1.3333	1.3333
Pitch moment of inertia, I_{yy}, slugs-ft^2	159.0	164.0
Yaw moment of inertia, I_{zz}, slugs-ft^2	159.0	164.0
Product of inertia, I_{xz}, slugs-ft^2	-0.31	-0.31
Pitch damping derivative, C_{m_q}, per radian	-110.0	-375.0
Yaw damping derivative, C_{n_r}, per radian	-110.0	-375.0

TABLE II
MAXIMUM FULL-SCALE POSITION UNCERTAINTIES RESULTING FROM BALANCE PRECISION LIMITATIONS

M_∞	t, sec	ΔX, ft	ΔY, ft	ΔZ, ft	$\Delta\theta$, deg	$\Delta\psi$, deg
0.66	0.3	±0.015	±0.015	±0.008	±0.15	±0.25
0.90	0.3	±0.032	±0.032	±0.016	±0.30	±0.52

UNCLASSIFIED

Security Classification

DOCUMENT CONTROL DATA - R & D

(Security classification of title, body of abstract and indexing annotation must be entered when the overall report is classified)

1. ORIGINATING ACTIVITY (Corporate author)	2a. REPORT SECURITY CLASSIFICATION
Arnold Engineering Development Center ARO, Inc., Operating Contractor Arnold Air Force Station, Tennessee	UNCLASSIFIED
	2b. GROUP N/A

3 REPORT TITLE

SEPARATION CHARACTERISTICS OF THE SUU-51 LASER-GUIDED DISPENSER MUNITION FROM THE F-4C AIRCRAFT

4 DESCRIPTIVE NOTES (Type of report and inclusive dates)

Final Report - April 16 to 19, 1971

5 AUTHOR(S) (First name, middle initial, last name)

Robert H. Roberts, ARO, Inc.

6. REPORT DATE	7a. TOTAL NO OF PAGES	7b. NO OF REFS
August 1971	58	1

8a. CONTRACT OR GRANT NO	9a. ORIGINATOR'S REPORT NUMBER(S)
F40600-72-C-0003 b. PROJECT NO 1120 c. Program Element 64724F d. Task 09	AEDC-TR-71-140 AFATL-TR-71-92 9b. OTHER REPORT NO(S) (Any other numbers that may be assigned this report) ARO-PWT-TR-71-101

10. DISTRIBUTION STATEMENT Distribution limited to U. S. Government agencies only; this report contains information on test and evaluation of military hardware; August 1971; other requests for this document must be referred to Armament Development and Test Center (DLGC), Eglin AFB, Florida 32542

11 SUPPLEMENTARY NOTES	12 SPONSORING MILITARY ACTIVITY
Available in DDC	Armament Development and Test Center (DLGC), Eglin AFB, Florida 32542

13. ABSTRACT Tests were conducted in the Aerodynamic Wind Tunnel (4T) using 0.05-scale models to investigate the separation characteristics of the SUU-51 Laser-Guided Dispenser Munition (LGDM) from Triple Ejection Rack and Multiple Ejection Rack locations on the inboard and centerline pylons, respectively, of the F-4C aircraft. Captive-trajectory store separation data were obtained at Mach numbers from 0.66 to 0.90, angles of attack from 0.3 to 2.1, and a simulated altitude of 5000 ft. At selected test conditions, parent-aircraft dive angles of 30 and 45 deg were simulated. Free-stream force and moment data were also obtained on the SUU-51 (LGDM) model at Mach numbers from 0.66 to 0.95 at store angles of attack from -6 to 20 deg. Generally, the store initially separated from the parent aircraft without store-to-parent contact. However, most of the trajectories were terminated after short time intervals because of a rapid pitch and yaw motion of the store. This termination was the result of limitations imposed by the test installation, such as sting-to-parent-aircraft contact, a store support system travel limit, or a balance load limit.

Distribution limited to U. S. Government agencies only; this report contains information on test and evaluation of military hardware; August 1971; other requests for this document must be referred to Armament Development and Test Center (DLGC), Eglin AFB, Florida 32542.

DD FORM 1 NOV 68 1473

UNCLASSIFIED

Security Classification

14. KEY WORDS	LINK A		LINK B		LINK C	
	ROLE	WT	ROLE	WT	ROLE	WT
F-4C aircraft						
external stores						
folding fins						
separation						
trajectories						
transonic flow						